Loops of Energy Bands for Bloch Waves in Optical Lattices

By Matt Coles and Dmitry Pelinovsky

We consider stationary Bloch waves in a Bose–Einstein condensate placed in a periodic potential for varying strengths of inter-atomic interactions. Bifurcations of the stationary states are known to occur in this context. These bifurcations generate loops in the energy bands of the Bloch waves near the ends and the center of the Brillouin zone. Using the method of Lyapunov–Schmidt reductions, we show that these bifurcations are of the supercritical pitchfork type. We also characterize the change in stability of the stationary states across the bifurcation point. Analytical results are illustrated by numerical computations.

1. Introduction

Bloch waves arise naturally when describing a particle in a periodic potential. Bloch's Theorem states that solutions to the linear Schrödinger equations in a periodic potential are given by quasi-periodic functions, which are now known as the Bloch functions [6]. Recent applications of nonlinear Bloch waves are known in photonic crystals and waveguide optics [16]. Periodic potentials induced by optical lattices are used to control Bose–Einstein condensates of ultra cold atomic gases [13]. Mathematical theory of Bloch functions and nonlinear localized stationary states in periodic potentials is constructed in the book [11].

In the context of cigar-shaped Bose–Einstein condensation, we consider the one-dimensional Gross–Pitaevskii equation as the mean-field model,

$$i\frac{\partial \Psi}{\partial t} = -\frac{\partial^2 \Psi}{\partial x^2} + V(x)\Psi + c|\Psi|^2\Psi, \tag{1}$$

Address for correspondence: Dmitry Pelinovsky, Department of Mathematics, McMaster University, Hamilton, Canada, ON L8S 4K1; e-mail: dmpeli@math.mcmaster.ca

DOI: 10.1111/j.1467-9590.2011.00536.x

STUDIES IN APPLIED MATHEMATICS 128:300–336

where $\Psi(x,t) : \mathbb{R} \times \mathbb{R} \to \mathbb{C}$ is the wave function of the condensate (with $|\Psi|^2$ being a probability density of Bose atoms), $V(x) : \mathbb{R} \to \mathbb{R}$ is the trapping potential, and $c \in \mathbb{R}$ is the strength of the inter-atomic interactions.

We take the potential V to be a 2π-periodic function, $V(x + 2\pi) = V(x)$. This potential corresponds to an optical lattice used for trapping the condensate. We deal both with the defocusing $c > 0$ and focusing $c < 0$ cases.

The main interest that draws our attention is the possibility of loops in the energy bands associated with the nonlinear Bloch waves. This possibility was first discovered by Wu and Niu (see their review in [17]) and later explored numerically by Machholm, Pethick, and Smith [7]. The loops were discovered in the defocusing case $c > 0$ for the lowest energy band near the end of the Brillouin zone and for the second energy band near the center of the Brillouin zone (see Figure 1 in [7]). For $V(x) = \cos(x)$, one can construct analytically the exact solutions for antiperiodic Bloch waves associated with the lowest energy band bifurcating at $c = 1$ to the interval $c > 1$ [1, 17].

More recently, loops in the energy bands for Bloch waves were discovered in the context of atomic Bloch–Zener oscillations in an optical cavity [14, 15]. This problem is modeled by the system of a linear Schrödinger equations for the atomic wave function and an evolution equation for the number of photons in the cavity [14]. The stationary Bloch waves satisfy the Schrödinger equations, where the nonlinear response is due to the coefficient in front of the periodic potential V. In this context, loops in the energy bands for Bloch waves bifurcate in the interior of the Brillouin zone and detach as new energy bands, in a sharp contrast from the energy bands for Bloch waves in optically trapped Bose–Einstein condensates.

The comparison between these two examples calls for systematic analysis of the loop bifurcations in the energy bands of the Bloch waves in periodic potentials. We study this phenomenon here, in the context of the Gross–Pitaevskii equation (1).

Our main results and the organization of this article are as follows. Section 2 contains the description of the energy bands for Bloch waves. We prove that the loops in the energy bands may only occur at the ends or the center of the Brillouin zone. Bifurcations like the one considered in [15] cannot occur within the Gross–Pitaevskii equation (1).

Section 3 presents asymptotic results on the energy bands for small values of the parameter c. Continuations with respect to parameter c are also performed numerically to illustrate existence of bifurcations of Bloch waves near the ends and the center of the Brillouin zone. We also prove that the only possible scenario of the relevant bifurcation at the lowest energy band is the appearance of complex-valued Bloch waves in addition to the real-valued Bloch wave that persists across the bifurcation point.

Section 4 contains the Lyapunov–Schmidt analysis of a general bifurcation of the stationary Bloch wave. We derive the normal form for this bifurcation,

which allows us to explain the appearance of the loop in the energy band. This normal form is valid both for the lowest energy band as well as for the higher energy bands assuming some constraints on the numerical coefficients.

The time-dependent normal form equation is derived in Section 5 to explain the change in stability of the stationary Bloch waves with respect to the time-dependent perturbations. For the lowest energy band, we prove that the upper branch of the loop that contains the real-valued Bloch wave is unstable with respect to the time-dependent perturbations, whereas the lower branches of the loop that contain complex-valued Bloch waves are stable.

Section 6 discusses the loop bifurcations in the context of atomic Bloch oscillations in optical cavities. Section 7 gives a summary of this work.

2. Energy bands for Bloch waves

The stationary states satisfy the time-independent Gross–Pitaevskii equation,

$$-\psi''(x) + V(x)\psi(x) + c|\psi(x)|^2\psi(x) = \mu\psi(x), \quad x \in \mathbb{R}, \tag{2}$$

where μ is an eigenvalue. Physically μ is associated with the chemical potential for the Bose–Einstein condensate. If we keep c as a free parameter, we should add the normalization condition,

$$Q(\psi) = \frac{1}{2\pi}\int_{-\pi}^{\pi} |\psi|^2 dx = 1. \tag{3}$$

Alternatively, we can normalize c and use $Q = Q(\psi)$ as a free parameter of the stationary states. The latter formalism is used in [8, 19] to characterize nonuniqueness of the Bloch waves and localized states in the periodic potentials. To avoid multiplicity of nonlinear Bloch waves, we shall normalize $Q(\psi) = 1$ and use c as a free parameter in what follows.

The Bloch waves are quasi-periodic solutions of the stationary equation (2),

$$\psi(x) = e^{ikx}\phi(x), \quad \phi(x + 2\pi) = \phi(x), \quad x \in \mathbb{R}, \tag{4}$$

where k is the Bloch wave number. Therefore,

$$\psi(x + 2\pi) = e^{2\pi ik + ikx}\phi(x + 2\pi) = e^{2\pi ik}\psi(x). \tag{5}$$

Due to the periodicity of the exponential term in (5) it is sufficient to consider k on the interval $[-\frac{1}{2}, \frac{1}{2}]$, called the Brillouin zone. The map $[-\frac{1}{2}, \frac{1}{2}] \ni k \mapsto \mu \in \mathbb{R}$ is called the energy band for the Bloch wave ψ satisfying (2) and (5). Both the Bloch wave and the energy band are 1-periodic in $k \in \mathbb{R}$, if they exist.

For $k = 0$, the Bloch wave is a 2π-periodic function, $\psi(x + 2\pi) = \psi(x)$. For $k = \pm\frac{1}{2}$, it is a 2π-antiperiodic function, $\psi(x + 2\pi) = -\psi(x)$. At either $k = 0$ or $k = \pm\frac{1}{2}$ the function ψ can be taken to be purely real because the stationary equation (2) admits a reduction to real-valued solutions and the

boundary conditions in (5) are real valued. We can not generally take ψ purely real for $k \neq \{0, \pm\frac{1}{2}\}$, as the boundary conditions in (5) are not real-valued.

Existence of the Bloch waves in the form (4) for small $c \in \mathbb{R}$ follows from the variational methods applied to the energy functional,

$$E_\mu(\psi) = \frac{1}{2\pi}\int_{-\pi}^{\pi}\left[|\psi'|^2 + V|\psi|^2 - \mu|\psi|^2 + \frac{1}{2}c|\psi|^4\right]dx, \quad \psi = e^{ikx}\phi, \quad \phi \in H^1_{\text{per}}(-\pi,\pi). \tag{6}$$

Variation of E_μ in ψ yields the stationary equation (2), where μ is the Lagrange multiplier of the variational problem subject to the normalization condition (3).

If $c = 0$, there exists a countable set of energy bands $\{\mu_n(k)\}_{n\in\mathbb{N}_0}$, where $\mathbb{N}_0 := \{0, 1, 2, 3, \ldots\}$ and $n = 0$ corresponds to the lowest energy band [4]. The lowest energy band achieves the minimum of E_μ under the constrained $Q(\psi) = 1$. The higher energy bands correspond to critical points of E_μ, which follows from the Courant's minimax principle.

If $V \in L^\infty$ and μ is taken in between values in the set $\{\mu_n(k)\}_{n\in\mathbb{N}_0}$ for any fixed $k \in [-\frac{1}{2}, \frac{1}{2}]$, Theorem 3.4 in [9] states that a critical point of E_μ exists for all $c \in \mathbb{R}$. The lowest energy band exists for $\mu < \mu_0(k)$ if $c < 0$ and for $\mu > \mu_0(k)$ if $c > 0$.

Let ψ be the family of Bloch waves of the stationary equation (2) for a fixed energy band with $k \in [-\frac{1}{2}, \frac{1}{2}]$. Integrating by parts we find that,

$$\mathcal{E}(k) := E_\mu(\phi e^{ikx}) = -\frac{c}{4\pi}\int_{-\pi}^{\pi}|\psi|^4 dx, \tag{7}$$

which yields,

$$\mu(k) = \frac{1}{2\pi}\int_{-\pi}^{\pi}[|\psi'|^2 + V|\psi|^2 + c|\psi|^4]dx, \tag{8}$$

Let us define a new function,

$$\mathcal{F}(k) := \mu - \frac{c}{4\pi}\int_{-\pi}^{\pi}|\psi|^4 dx \equiv \mu(k) + \mathcal{E}(k), \tag{9}$$

We will show that $\mathcal{F}(k)$ is monotonically increasing or decreasing for any $k \in (-\frac{1}{2}, 0) \cup (0, \frac{1}{2})$. Because the same properties hold for the energy band function $\mu(k)$ in the linear limit $c = 0$, these results show that $\mathcal{F}(k)$ can be used as the *nonlinear energy band function*.

LEMMA 1. *For a fixed $c \in \mathbb{R}$, let ψ be a family of critical points of $E_\mu(\psi)$ subject to $Q(\psi) = 1$ in the form of the Bloch wave (5) with $\phi \in H^1_{\text{per}}(-\pi, \pi)$ and $k \in [-\frac{1}{2}, \frac{1}{2}]$. Then, $\mathcal{F}(k)$ defined by (9) is a C^1 function of k for all $k \in (-\frac{1}{2}, 0) \cup (0, \frac{1}{2})$such that $\mathcal{F}'(k) \neq 0$.*

Proof: Let $\psi = e^{ikx}\phi$ with $\phi \in H^1_{\text{per}}(-\pi, \pi)$ be a critical point of $E_\mu(\psi)$ for some $\mu(k)$. The energy functional (6) yields the Euler–Lagrange equation,

$$-\phi''(x) - 2ik\phi'(x) + (V(x) + k^2 - \mu(k) + c|\phi(x)|^2)\,\phi(x) = 0. \tag{10}$$

By the bootstrapping arguments, if $\phi \in H^1_{\text{per}}(-\pi, \pi)$ and $V \in L^\infty(\mathbb{R})$, then $\phi \in H^2_{\text{per}}(-\pi, \pi)$. By the Sobolev embedding of $H^2_{\text{per}}(-\pi, \pi)$ to $C^1_{\text{per}}(-\pi, \pi)$, we have $\phi \in C^1_{\text{per}}(-\pi, \pi)$.

The stationary equation (2) yields the first integral,

$$\begin{aligned} \frac{d}{dx}(-\bar\psi\psi' + \psi\bar\psi') = 0 \;\Rightarrow\; C_0 &= i(-\bar\psi\psi' + \psi\bar\psi') \\ &= i(-\bar\phi\phi' + \phi\bar\phi') + 2k|\phi|^2 = \text{const}. \end{aligned} \tag{11}$$

We note that $C_0 \neq 0$ if $k \neq \{0, \pm\frac{1}{2}\}$ because if $C_0 = 0$, then ψ and $\bar\psi$ are constant proportional to each other with the constant to be ± 1 (for $c \neq 0$). However, the constraint $\psi = \bar\psi$ is impossible, because $\psi(2\pi) = e^{2\pi ik}\psi(0)$ and even if $\psi(0) \in \mathbb{R}$, then $\psi(2\pi) \notin \mathbb{R}$ if $k \neq \{0, \pm\frac{1}{2}\}$ (similarly, constraint $\psi = -\bar\psi$ is also impossible).

Continuity of $\phi \in H^2_{\text{per}}(\mathbb{R})$ and $\mu \in \mathbb{R}$ with respect to parameter k for all $k \in (-\frac{1}{2}, 0) \cup (0, \frac{1}{2})$ follows from the continuous dependence of solutions of the differential equation (10) and the energy functional (8) from the parameter k, thanks to the compact Sobolev embedding of $H^2_{\text{per}}(-\pi, \pi)$ to $L^4_{\text{per}}(-\pi, \pi)$. Now we consider differentiability of ϕ and μ with respect k from the derivative equation,

$$\left(-\partial_x^2 + V - \mu\right)\partial_k\psi = \psi\,\partial_k\mu - 2c|\psi|^2\partial_k\psi - c\psi^2\partial_k\bar\psi. \tag{12}$$

Multiplying this equation to ψ and integrating twice by parts, we obtain,

$$\begin{aligned} \partial_k\mu \int_{-\pi}^{\pi} |\psi|^2 dx - c\int_{-\pi}^{\pi} |\psi|^2(\bar\psi\,\partial_k\psi + \psi\,\partial_k\bar\psi)dx \\ = [(\partial_x\bar\psi)(\partial_k\psi) - \bar\psi\,\partial_k\partial_x\psi]\big|_{x=-\pi}^{x=\pi} \\ = 2\pi[i(-\bar\phi\phi' + \phi\bar\phi') + 2k|\phi|^2]|_{x=\pi} = 2\pi C_0, \end{aligned} \tag{13}$$

where boundary conditions (5) and the first invariant (11) are used for the last equality. Because C_0 is continuous in k and nonzero for all $k \in (-\frac{1}{2}, 0) \cup (0, \frac{1}{2})$, it follows from (13) that $\mathcal{F}(k)$ is continuously differentiable in k with $\mathcal{F}'(k) \neq 0$ for all $k \in (-\frac{1}{2}, 0) \cup (0, \frac{1}{2})$. □

Because $\mathcal{F}(k)$ and $\mu(k)$ are C^1 functions for all $k \in (-\frac{1}{2}, 0) \cup (0, \frac{1}{2})$, loops and new branches of Bloch waves may only occur either at the end points $k = \pm\frac{1}{2}$ or the center $k = 0$ of the Brillouin zone. At the end points $k = \pm\frac{1}{2}$, $\mu'(k)$ is zero for $c = 0$ and remain zero for small values of $c \in \mathbb{R}$, providing smoothness of a global 1-periodic extension of $\mu(k)$ over $k \in \mathbb{R}$. However,

for some values of $c \in \mathbb{R}$, $\mu'(k)$ may be nonzero at $k = \pm\frac{1}{2}$, which would indicate the loss of smoothness in the global 1-periodic extension of $\mu(k)$ over $k \in \mathbb{R}$ and the possibility of other energy bands centered at $k = \pm\frac{1}{2}$. These are the loop bifurcations of the energy bands, which we are studying in this paper. Additionally, if a periodic minimizer in a minimax variational principle becomes degenerate, the loop in the energy band may bifurcate at the center $k = 0$ of the Brillouin zone. We show numerically that this indeed happens for the second energy band if $c > 0$.

3. Energy bands for small values of c

Because loop bifurcations occur at the end or center points of the Brillouin zone, we consider the Bloch waves at $k = 0$ and $k = \frac{1}{2}$. In what follows, we give details for the case $k = \frac{1}{2}$, whereas the case $k = 0$ is fully analogous. When $k = \frac{1}{2}$, the corresponding Bloch wave ψ satisfying the stationary Gross–Pitaevskii equation (2) is a 2π-antiperiodic function.

The linear analogue of the stationary Gross–Pitaevskii equation,

$$-\psi''(x) + V(x)\psi = \mu\psi, \quad \psi(x + 2\pi) = -\psi(x), \tag{14}$$

admits a countable set of eigenvalues $\{\mu_n\}_{n\in\mathbb{N}_0}$, where $\mathbb{N}_0 := (0, 1, 2, \ldots)$, at discrete energy levels, each with a corresponding wave function, $\psi_n \in \mathcal{H}^2_{a.p.}$, where,

$$\mathcal{H}^2_{a.p.} := \{f \in H^2([-\pi, \pi], \mathbb{R}) : \quad f(-\pi) = -f(\pi), \ f'(-\pi) = -f'(\pi)\}. \tag{15}$$

We take each ψ_n to be real and normalized by $\|\psi_n\|_{L^2} = 1$ where,

$$\|f\|^2_{L^2} := \langle f, f\rangle_{L^2}, \quad \langle f, g\rangle_{L^2} := \frac{1}{2\pi}\int_{-\pi}^{\pi} f(x)g(x)dx, \tag{16}$$

and the factor $\frac{1}{2\pi}$ is included for convenience of normalization. The following theorem states that any linear Bloch wave can be uniquely continued as a solution of the stationary Gross–Pitaevskii equation (2) for small $c \in \mathbb{R}$.

THEOREM 1. *Fix $n \in \mathbb{N}_0$ such that $\mu_m \neq \mu_n$ for all $m \in \mathbb{N}_0\backslash\{n\}$. There exists $c_n > 0$ and $D_1, D_2 > 0$ such that for any $c \in (-c_n, c_n)$, the stationary Gross–Pitaevskii equation,*

$$-\psi'' + V(x)\psi + c\psi^3 = \mu\psi, \quad \psi(x + 2\pi) = -\psi(x), \quad \|\psi\|_{L^2} = 1, \tag{17}$$

admits a unique branch of Bloch waves satisfying,

$$|\mu - \mu_n| \leq D_1 c, \quad \|\psi - \psi_n\|_{H^2} \leq D_2 c.$$

We outline a standard method to prove the theorem in Section 3.1.

Loop bifurcations of Bloch bands centered at $k = \frac{1}{2}$ are determined by the change in the number of negative eigenvalues of the linear Schrödinger operators,

$$L_+ := -\partial_x^2 + V(x) + 3c\psi^2(x) - \mu, \tag{18}$$

$$L_- := -\partial_x^2 + V(x) + c\psi^2(x) - \mu, \tag{19}$$

where ψ is the antiperiodic Bloch wave of the stationary equation (17) that corresponds to the nonlinear eigenvalue μ. Operator L_+ can be obtained by differentiating the stationary Gross–Pitaevskii equation (2) with respect to real ψ. Differentiating (2) with respect to imaginary ψ yields operator L_-. Eigenvalues of $L_\pm$ for small $c \in \mathbb{R}$ are approximated in Section 3.2.

Numerical approximations in comparison with the asymptotic results are given in Section 3.3.

3.1 Bloch waves for small c

Let us pick $\psi_n \in \mathcal{H}^2_{a.p.}$ and μ_n satisfying the linear equation (14) for some $n \in \mathbb{N}_0$. We assume that,

$$\mu_m \neq \mu_n \quad \text{for all} \quad m \in \mathbb{N}_0 \backslash \{n\}, \tag{20}$$

which means that the two adjacent spectral bands for the Bloch waves are disjoint. It is clear that $\text{Ker}(L_n) = \text{span}(\psi_n)$ where,

$$L_n := -\partial_x^2 + V(x) - \mu_n, \tag{21}$$

is an unbounded operator from $\mathcal{H}^2_{a.p.}$ to $L^2_{a.p.}$. Because L_n is self-adjoint, its kernel and range are orthogonal so,

$$\text{Ran}(L_n) = \left\{ f \in L^2_{a.p.} : \quad \langle f, \psi_n \rangle_{L^2} = 0 \right\}. \tag{22}$$

Therefore, it is natural to introduce the decomposition, $L^2 = \{\psi_n\} \oplus \text{Ran}(L_n)$ and define the projection operator, $P_n : L^2 \to \text{Ran}(L_n)$. Standard methods based on eigenfunction decompositions show that if the nonresonance condition (20) is satisfied then,

$$\left\| P_n L_n^{-1} P_n \right\|_{H^2 \to H^2} \leq \sup_{m \in \mathbb{N}_0 \backslash \{n\}} \frac{1}{|\mu_m - \mu_n|} =: N < \infty. \tag{23}$$

We consider a solution ψ of the stationary equation (17) with nonlinear eigenvalue μ and decompose,

$$\mu = \mu_n + \delta\mu, \quad \psi = a\psi_n + \delta\psi, \quad a \in \mathbb{R}, \quad \langle \psi_n, \delta\psi \rangle_{L^2} = 0. \tag{24}$$

Then, equation (17) is rewritten as,

$$L_n \delta\psi = \mathcal{F} \equiv \delta\mu(a\psi_n + \delta\psi) - c(a\psi_n + \delta\psi)^3. \tag{25}$$

Right-hand side term $\mathcal{F}$ must be in the range of L_n, thus it follows that,

$$\begin{aligned}\langle \delta\mu(a\psi_n + \delta\psi) - c(a\psi_n + \delta\psi)^3, \psi_n\rangle_{L^2} &= 0 \\ \Rightarrow \delta\mu &= \frac{c}{a}\langle (a\psi_n + \delta\psi)^3, \psi_n\rangle_{L^2}.\end{aligned} \tag{26}$$

On the other hand, the normalization of ψ and ψ_n gives,

$$1 = a^2 + \|\delta\psi\|_{L^2}^2 \Rightarrow a = \sqrt{1 - \|\delta\psi\|_{L^2}^2}. \tag{27}$$

If we can prove that $\|\delta\psi\|_{H^2} = \mathcal{O}(c)$ then we have,

$$a = 1 + \mathcal{O}(c^2), \quad \delta\mu = c\|\psi_n\|_{L^4}^4 + \mathcal{O}(c^2), \tag{28}$$

and the proof of Theorem 1 is complete.

We now turn our attention to $\delta\psi$, which solves the fixed-point problem,

$$\delta\psi = \left(P_n L_n^{-1} P_n\right)\mathcal{F} = \left(P_n L_n^{-1} P_n\right)(\delta\mu(a\psi_n + \delta\psi) - c(a\psi_n + \delta\psi)^3) \equiv \mathcal{A}(\delta\psi; c). \tag{29}$$

The nonlinear operator $\mathcal{A}$ depends only on $\delta\psi \in \mathcal{H}^2_{a.p.}$ and $c \in \mathbb{R}$ since $\delta\mu$ and a are uniquely determined by constraint (26) and normalization (27). The following lemma guarantees a small solution of the fixed-point equation (29) such that the condition $\|\delta\psi\|_{H^2} = \mathcal{O}(c)$ is satisfied.

LEMMA 2. *There is $c_n > 0$ and $D > 0$ such that for any $c \in (-c_n, c_n)$, the nonlinear operator $\mathcal{A}(\delta\psi; c)$, as defined by* (26), (27), *and* (29), *has a unique fixed point, $\delta\psi \in \mathcal{H}^2_{a.p.}$, in a neighborhood of $0 \in \mathcal{H}^2_{a.p.}$ satisfying $\|\delta\psi\|_{H^2} \le Dc$.*

Proof: We will apply the Banach Fixed Point Theorem (see Section 1.6 in [20] for a precise statement) to the proof of existence and uniqueness of a fixed point of $\mathcal{A}$. We must show that $\mathcal{A}$ maps a closed neighborhood around $0 \in \mathcal{H}^2_{a.p.}$ into itself and that $\mathcal{A}$ is a contraction map. Take $\bar{\mathcal{B}}_\varepsilon \subset \mathcal{H}^2_{a.p.}$ with,

$$\bar{\mathcal{B}}_\varepsilon := \left\{\psi \in \mathcal{H}^2_{a.p.} : \|\psi\|_{H^2} \le \varepsilon\right\}, \tag{30}$$

a closed neighborhood around $0 \in \mathcal{H}^2_{a.p.}$. Take $\delta\psi \in \bar{\mathcal{B}}_\varepsilon$ and consider the norm of $\mathcal{A}(\delta\psi; c)$ for small c. Note that $\psi_n \in \mathcal{H}^2_{a.p.}$ gives $\|\psi_n\|_{H^2} \le R$ for some $R > 0$.

We will use the Banach algebra property of H^2: for any $f, g \in H^2$, there is $K > 0$ such that,

$$\|fg\|_{H^2} \le K\|f\|_{H^2}\|g\|_{H^2}. \tag{31}$$

Using (23) and (31) we have,

$$\begin{aligned}\|\mathcal{A}(\delta\psi;c)\|_{H^2} &= \|P_nL_n^{-1}P_n\|_{H^2\to H^2}\|\delta\mu(a\psi_n+\delta\psi)-c(a\psi_n+\delta\psi)^3\|_{H^2}\\ &\le N(R|a||\delta\mu|+|\delta\mu|\varepsilon+cK^2(R^3|a|^3+3R^2|a|^2\varepsilon\\ &\quad +3R|a|\varepsilon^2+\varepsilon^3)).\end{aligned}\tag{32}$$

Because $|\delta\mu|=\mathcal{O}(c)$ from (26) if $\delta\psi\in\bar{\mathcal{B}}_\varepsilon$, there is a $c_n>0$ such that for all $c\in(-c_n,c_n)$, there is $\varepsilon=\varepsilon(c)$ such that $\|\mathcal{A}(\delta\psi;c)\|_{H^2}\le\varepsilon$ if $\|\delta\psi\|_{H^2}\le\varepsilon$. Hence, $\mathcal{A}$ maps a closed ball in $\mathcal{H}^2_{a.p.}$ into itself.

Now we show that $\mathcal{A}$ is a contraction map for small c. That is, we need to show that there is $c_n>0$ such that for all $c\in(-c_n,c_n)$ there is $q=q(c)$ such that $q\in(0,1)$ and,

$$\|\mathcal{A}(\delta\psi_1;c)-\mathcal{A}(\delta\psi_2;c)\|_{H^2}\le q\|\delta\psi_1-\delta\psi_2\|_{H^2},\tag{33}$$

where,

$$\begin{aligned}\mathcal{A}(\delta\psi_1;c)-\mathcal{A}(\delta\psi_2;c)=&P_nL_n^{-1}P_n\big((\delta\mu_1a_1-\delta\mu_2a_2)\psi_n+\delta\mu_1\delta\psi_1\\ &-\delta\mu_2\delta\psi_2-c\big(\big(a_1^3-a_2^3\big)\psi_n^3+3\psi_n^2\big(a_1^2\delta\psi_1-a_2^2\delta\psi_2\big)\\ &+3\psi_n\big(a_1\delta\psi_1^2-a_2\delta\psi_2^2\big)+\big(\delta\psi_1^3-\delta\psi_2^3\big)\big)\big).\end{aligned}\tag{34}$$

Lengthy but straightforward computations (see [3] for details) show that there are (c,ε)-independent constants M_0, M_1, $M_2>0$ such that for small c and finite $\varepsilon>0$ we have,

$$q:=|c|N\big(M_0+M_1\varepsilon+M_2\varepsilon^2\big).\tag{35}$$

It is clear that there exists $c_n>0$ such that $q<1$ for all $c\in(-c_n,c_n)$ and thus $\mathcal{A}$ is a contraction mapping. Thus, by the Banach Fixed Point Theorem [20], we have the existence of a unique fixed point, $\delta\psi\in\mathcal{H}^2_{a.p.}$, of $\mathcal{A}$ for sufficiently small c.

It remains to estimate the magnitude of $\delta\psi$ for small c. Expansion of (26), (27), and (29) gives,

$$\delta\psi=c\big(P_nL_n^{-1}P_n\big)\big(\|\psi_n\|_{L^4}^4\psi_n-\psi_n^3+\mathcal{O}(\|\delta\psi\|_{H^2})\big).\tag{36}$$

If $\delta\psi$ is a unique fixed point of the fixed-point problem (29) for small c, then (36) gives,

$$\delta\psi=c\big(P_nL_n^{-1}P_n\big)\big(\|\psi_n\|_{L^4}^4\psi_n-\psi_n^3\big)+\mathcal{O}(c^2),\tag{37}$$

so that there is $D>0$ such that $\|\delta\psi\|_{H^2}\le Dc$. □

We refer to the unique continuation of the Bloch wave in Theorem 1 as the *stationary real branch*. Note that the above argument applies equally well for periodic boundary conditions in the stationary system (17), that is for, $k=0$

with $\psi \in \mathcal{H}^2_p$ where,

$$\mathcal{H}^2_p := \{f \in H^2([-\pi,\pi],\mathbb{R}) : f(-\pi) = f(\pi),\ f'(-\pi) = f'(\pi)\}. \tag{38}$$

In fact, a unique continuation of Bloch waves in c can be proven for all $k \in [-\frac{1}{2}, \frac{1}{2}]$. Of course the result of Theorem 1 only holds in a neighborhood of small c. A further increase in c may lead to a change in the number of solutions of the stationary equation (2).

3.2 Linearized operators for small c

If ψ is a Bloch wave satisfying the stationary equation (17) in Theorem 1, then $L_-\psi = 0$, where L_- is a linear operator in (19). Because we are interested in bifurcations of stationary solutions, we examine the eigenvalues of $L_\pm$ and look for a change in the number of negative eigenvalues. Using the asymptotic approximation in Theorem 1, we can approximate eigenvalues of $L_\pm$ for small c.

Let $\mu(c)$ denote a particular stationary real branch with the Bloch wave ψ originating from the linear eigenmode ψ_n for some $n \in \mathbb{N}_0$. Using (28) we obtain,

$$\mu'(0) = \lim_{c\to 0} \frac{\mu - \mu_n}{c} = \|\psi_n\|^4_{L^4}. \tag{39}$$

Now consider linearized operators $L_\pm(c)$ and their eigenvalues along the stationary real branch. Denote the eigenvalues of $L_\pm(c)$ by $\lambda^{(m)}_\pm(c)$, $m \in \mathbb{N}_0$ and their L^2 normalized eigenfunctions $\varphi^{(m)}_\pm$. The Rayleigh quotient gives,

$$\lambda^{(m)}_\pm(c) = \left\langle L_\pm(c)\varphi^{(m)}_\pm, \varphi^{(m)}_\pm \right\rangle_{L^2}. \tag{40}$$

Because $L_+(0) = L_-(0) \equiv L_n = -\partial_x^2 + V(x) - \mu_n$ have eigenvalues $\lambda^{(m)}_\pm(0) = \mu_m - \mu_n$ with normalized eigenfunctions ψ_m we obtain,

$$\begin{aligned}
(\lambda^{(m)}_+)'(0) &= 3\left\langle \psi_n^2, \psi_m^2 \right\rangle_{L^2} - \|\psi_n\|^4_{L^4}, \\
(\lambda^{(m)}_-)'(0) &= \langle \psi_n^2, \psi_m^2 \rangle_{L^2} - \|\psi_n\|^4_{L^4}.
\end{aligned} \tag{41}$$

We recall that $L_\pm(0) = L_n$ has a simple zero eigenvalue and n negative eigenvalues. The rest of the purely discrete spectrum of $L_\pm(0)$ is strictly positive. Since,

$$\left(\lambda^{(n)}_+\right)'(0) = 2\|\psi_n\|^4_{L^4} > 0, \quad \left(\lambda^{(n)}_-\right)'(0) = 0, \tag{42}$$

operator $L_+(c)$ has n negative and no zero eigenvalues for small $c > 0$ and $(n+1)$ negative and no zero eigenvalues for small $c < 0$, whereas operator L_- has n negative and one zero eigenvalue for small $c \neq 0$ (recall that $L_-(c)\psi = 0$ for any $c \in \mathbb{R}$).

The above count holds for small values of c. If in addition, $c > 0$, the following lemma states that the number of negative eigenvalues of $L_+(c)$

cannot exceed the number of negative eigenvalues of $L_-(c)$. This result is rather abstract and holds for large positive values of c as well.

LEMMA 3. *Assume that the spectrum of $L_-(c)$ has $\kappa(c)$ negative eigenvalues and a simple zero eigenvalue. If $c > 0$, the spectrum of $L_+(c)$ has at most $\kappa(c)$ nonpositive eigenvalues accounting their multiplicity.*

Proof: It is clear from (18) and (19) that,

$$L_+(c) = L_-(c) + 2c\psi^2.$$

Note that since $L_+(c)$ and $L_-(c)$ are self-adjoint, their eigenfunctions form an orthogonal basis for $\mathcal{H}^2_{a.p.}$. For the negative and zero eigenvalues of $L_-(c)$, we write,

$$L_-(c)u_m = \nu_m(c)u_m, \quad 0 \le m \le \kappa(c), \tag{43}$$

where the ordering $\nu_{\kappa(c)}(c) \le \nu_{\kappa(c)-1}(c) \le \cdots \le \nu_0(c) = 0$ includes eigenvalues with multiplicity greater than one. Similarly, for $L_+(c)$, we write,

$$L_+(c)w_m = \gamma_m(c)w_m, \quad 1 \le m \le M, \tag{44}$$

where, $\gamma_M(c) \le \gamma_{M-1}(c) \le \cdots \le \gamma_1(c) \le 0$. We claim that $M \le \kappa(c)$. Suppose $M > \kappa(c)$ and derive a contradiction. For $f \in \text{span}\{w_1, \ldots w_M\}$ we write,

$$f = \sum_{m=1}^{M} c_m w_m, \tag{45}$$

for some coefficients and note that,

$$\langle L_+(c)f, f\rangle_{L^2} = \sum_{m=1}^{M} |c_m|^2 \gamma_m(c) \le 0, \tag{46}$$

because of the orthogonality of eigenfunctions $\{w_m\}_{m=1}^M$. Now let us write $\{w_m\}_{m=1}^M$ as an orthogonal decomposition over eigenfunctions of $L_-(c)$,

$$w_m = \sum_{l=1}^{\kappa(c)} a_{m,l}u_m + \widetilde{w}_m, \quad \widetilde{w}_m \perp \text{span}\{u_1, \ldots, u_{\kappa(c)}\}, \tag{47}$$

with $\langle L_-(c)\widetilde{w}_m, \widetilde{w}_m\rangle_{L^2} \ge 0$. Consider,

$$g = \sum_{m=1}^{M} b_m w_m + \widetilde{g} = \sum_{l=1}^{\kappa(c)} \left(\sum_{m=1}^{M} a_{m,l} b_m \right) u_l + \widetilde{g} + \sum_{m=1}^{M} b_m \widetilde{w}_m, \tag{48}$$

where $\widetilde{g} \perp \text{span}\{u_1, \ldots, u_{\kappa(c)}\}$. If $g = 0$, then the expansion (48) represents a decomposition of 0 over eigenfunctions of L_- so that,

$$\widetilde{g} = -\sum_{m=1}^{M} b_m \widetilde{w}_m = -\sum_{m=1}^{M} b_m w_m, \tag{49}$$

and,

$$\sum_{m=1}^{M} a_{m,l} b_m = 0, \quad 1 \le l \le \kappa(c). \tag{50}$$

If $M > \kappa(c)$, then the linear system (50) is under-determined and there exists a nonzero solution for $\{b_1, \ldots, b_M\}$. Therefore, $\widetilde{g}$ in (49) is a nonzero vector. Since $\widetilde{g} \in \text{span}\{w_1, \ldots, w_M\}$ the quadratic form (46) gives,

$$\langle L_+(c)\widetilde{g}, \widetilde{g}\rangle_{L^2} = \sum_{m=1}^{M} |b_m|^2 \gamma_m(c) \le 0.$$

On the other hand, since $\widetilde{g} \in \text{span}\{\widetilde{w}_1, \ldots, \widetilde{w}_M\} \perp \text{span}\{u_1, \ldots, u_{\kappa(c)}\}$ and $\widetilde{g} \neq 0$ we have $\langle L_-(c)\widetilde{g}, \widetilde{g}\rangle_{L^2} \ge 0$ and,

$$\langle L_+(c)\widetilde{g}, \widetilde{g}\rangle_{L^2} = \langle L_-(c)\widetilde{g}, \widetilde{g}\rangle_{L^2} + 2c\langle \psi^2, \widetilde{g}^2\rangle_{L^2} > 0.$$

A contradiction shows that $M \le \kappa(c)$. □

COROLLARY 1. *Assume that $\kappa(0) = 0$. Because $c > 0$ increases, the first eigenvalue that crosses zero may only occur in the operator $L_-(c)$.*

Proof: If $\kappa(0) = 0$, then the spectrum of $L_+(c)$ is positive definite for small $c > 0$. It will remain positive definite for all values of $c > 0$, for which $\kappa(c) = 0$. However, once $\kappa(c)$ jumps from 0 to 1, it means that the spectrum of $L_-(c)$ acquired a negative eigenvalue by crossing the zero eigenvalue (which always exists in the spectrum of $L_-(c)$). □

Corollary 1 is applied to the lowest energy band, for which $\kappa(c) = 0$ holds always for small values of c.

3.3 Numerical approximations of Bloch waves

In order to construct numerical approximations of the Bloch waves ψ (for $k = 0$ and $k = \frac{1}{2}$) we solve the second-order differential equation,

$$-\phi''(x) + V(x)\phi \pm \phi^3 = \mu\phi, \quad x \in [-\pi, \pi], \tag{51}$$

with continuous parameter μ. We solve the differential equation (51) using a shooting method by taking advantage of the boundary conditions: $\phi(x + 2\pi) = -\phi(x)$ for $k = \frac{1}{2}$ or $\phi(x + 2\pi) = \phi(x)$ for $k = 0$. Once we have ϕ for a given value

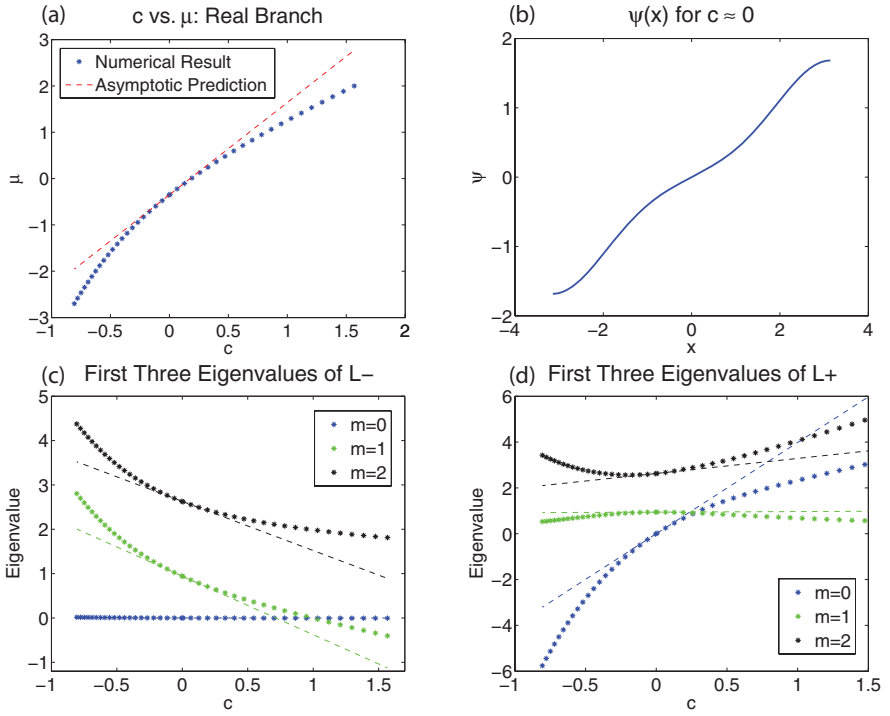

Figure 1. Numerical results for $k = \frac{1}{2}$, $n = 0$ (astrix) and asymptotic approximations (dashed lines): (a) Dependence of μ versus c for the stationary real branch, (b) Wave function ψ close to $c = 0$, (c) Eigenvalues of $L_-(c)$, and (d) Eigenvalues of $L_+(c)$. Note the change in sign of the eigenvalue with $m = 1$ of $L_-(c)$ at $c = 1$.

of μ, we compute c and ψ in the stationary Gross–Pitaevskii equation (2) by,

$$\psi = \frac{1}{\sqrt{N}}\phi, \quad c = \pm N, \tag{52}$$

where $N = \|\phi\|_{L^2}^2$. The different signs correspond to the positive and negative values of c.

Once we have determined c and ψ we have operators $L_\pm(c)$ and can numerically approximate their eigenvalues. In the figures that follow we use $V(x) = \cos(x)$ as the potential of the stationary system (17). Note that in Figure 1 (c) the bifurcation at $c = 1$ is exactly the loop bifurcation mentioned in [17].

The most interesting aspect of Figures 1–6 are the values of c for which the number of negative eigenvalues of $L_-(c)$ changes. This phenomenon is seen in Figure 1 (at $c = 1$), Figure 3 (around $c = 0.05$), Figure 5 (around $c = 0.4$), and Figure 6 (around $c = -0.3$).

No change in the number of negative eigenvalues is observed for operator $L_+(c)$. The change in the number of negative eigenvalues of $L_-(c)$ leads to a

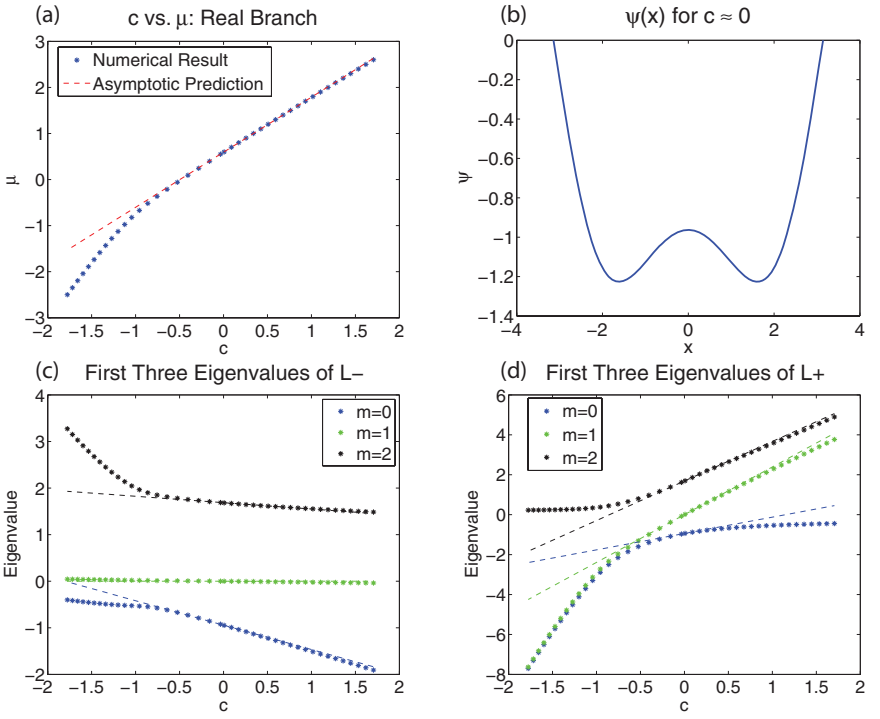

Figure 2. Similar to Figure 1 but with $k = \frac{1}{2}$ and $n = 1$.

bifurcation of the stationary Bloch waves. We analyse this bifurcation in the next section.

4. Loop bifurcations of Bloch bands

Here, we consider only the case $k = \frac{1}{2}$ for simplicity. We pick a stationary real branch for some fixed $n \in \mathbb{N}_0$. Recall that for small c, operator $L_+(c)$ is invertible and operator $L_-(c)$ has a one-dimensional kernel spanned by ψ. We assume that $L_+(c)$ remains invertible for larger values of c but the kernel of $L_-(c)$ becomes two-dimensional for a particular value of $c = c_*$. Examples of this occur in Figure 1 and Figure 3 for $k = \frac{1}{2}$. We denote $\mu_* := \mu_n(c_*)$, $\psi_* := \psi$ and,

$$L_+^* := -\partial_x^2 + V(x) + 3c_*\psi_*^2(x) - \mu_*, \tag{53}$$

$$L_-^* := -\partial_x^2 + V(x) + c_*\psi_*^2(x) - \mu_*. \tag{54}$$

Recall that $L_-^*\psi_* = 0$. We then define the bifurcation at $c = c_*$ according to the following two conditions,

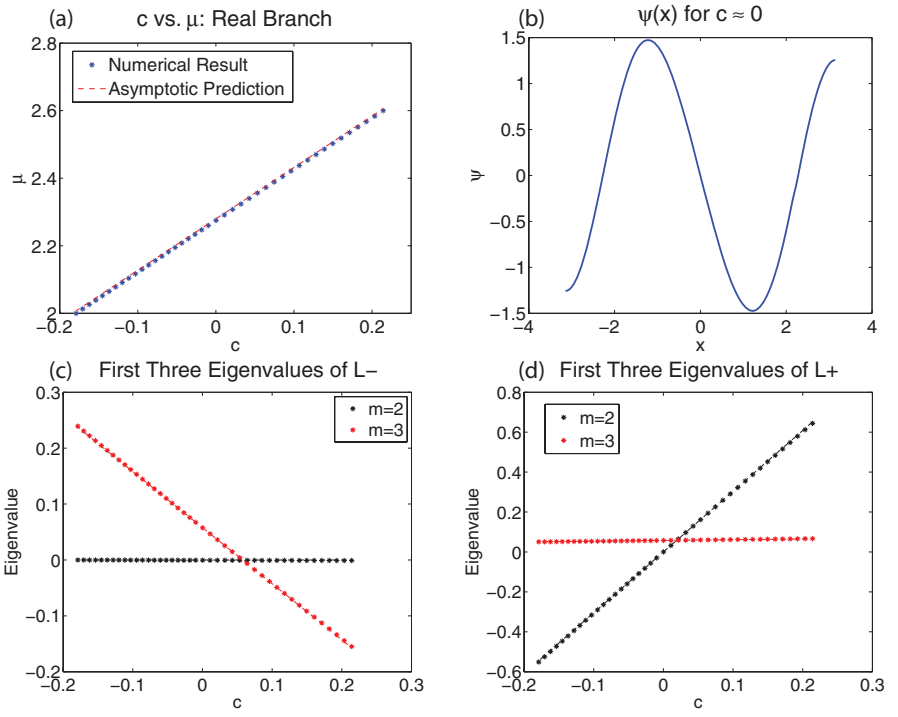

Figure 3. Similar to Figure 1 but with $k = \frac{1}{2}$ and $n = 2$. Note the change in sign of the eigenvalue with $m = 3$ of $L_{-}(c)$ at $c \approx 0.05$.

(A1) L_{+}^{*} is invertible

(A2) $\exists\, \varphi_{*} \in \mathcal{H}^{2}_{a.p.}$ such that $L_{-}^{*}\varphi_{*} = 0$ and $\langle \varphi_{*}, \psi_{*} \rangle_{L^2} = 0$.

The following theorem describes the details of this bifurcation, which is seen to be the pitchfork (symmetry-breaking) bifurcation.

THEOREM 2. *Assume that (A1) and (A2) hold. Suppose that,*

$$
\begin{aligned}
S_0 &\equiv \langle \psi_{*}, (L_{+}^{*})^{-1}\psi_{*} \rangle_{L^2} \neq 0, \\
P_0 &\equiv -\langle \psi_{*}^{2}, \varphi_{*}^{2} \rangle_{L^2} + 2c_{*}\langle \psi_{*}\varphi_{*}^{2}, (L_{+}^{*})^{-1}\psi_{*}^{3} \rangle_{L^2} \\
&\quad + \alpha_0\big(1 - 2c_{*}\langle \psi_{*}\varphi_{*}^{2}, (L_{+}^{*})^{-1}\psi_{*} \rangle_{L^2}\big) \neq 0, \\
Q_0 &\equiv c_{*}\big(2c_{*}\langle \psi_{*}\varphi_{*}^{2}, (L_{+}^{*})^{-1}\varphi_{*}^{2}\psi_{*} \rangle_{L^2} - \|\varphi_{*}\|_{L^4}^{4}\big) \\
&\quad + \beta_0\big(1 - 2c_{*}\langle \psi_{*}\varphi_{*}^{2}, (L_{+}^{*})^{-1}\psi_{*} \rangle_{L^2}\big) \neq 0, \\
R_0 &\equiv 2\langle \psi_{*}', \varphi_{*} \rangle_{L^2} \neq 0,
\end{aligned}
$$

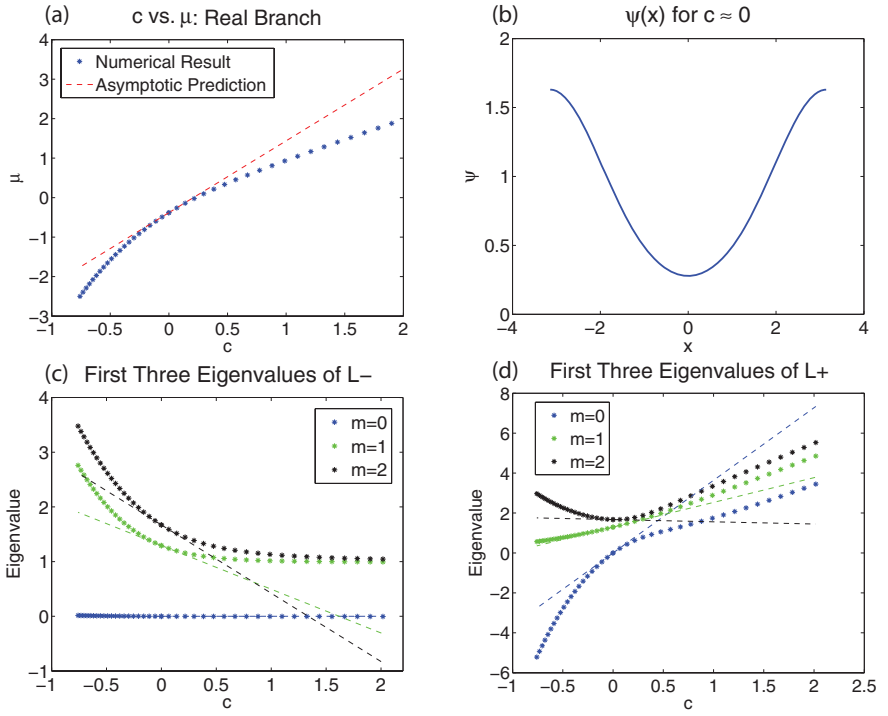

Figure 4. Similar to Figure 1 but with $k = 0$ and $n = 0$.

where,

$$\alpha_0 \equiv \frac{\langle \psi_*, (L_+^*)^{-1}\psi_*^3\rangle_{L^2}}{\langle \psi_*, (L_+^*)^{-1}\psi_*\rangle_{L^2}}, \qquad \beta_0 \equiv \frac{2c_*\langle \psi_*, (L_+^*)^{-1}\varphi_*^2\psi_*\rangle_{L^2} - 1}{2\langle \psi_*, (L_+^*)^{-1}\psi_*\rangle_{L^2}}.$$

If $\mathrm{sign}(P_0Q_0) = -1$, *there exists* $\varepsilon_0 > 0$, $\delta > 0$, *and* $\eta > 0$ *such that the stationary Gross–Pitaevskii equation (2) with* $c = c_* + \varepsilon$ *admits a unique Bloch wave solution (5) for all* $\varepsilon \in (-\varepsilon_0, 0]$ *and* $|k - \frac{1}{2}| < \delta$ *and three Bloch wave solutions (5) for all* $\varepsilon \in (0, \varepsilon_0)$ *and* $|k - \frac{1}{2}| < \eta\varepsilon^{3/2}$.

Remark 1. If $\mathrm{sign}(P_0Q_0) = +1$, the ε neighbourhoods are reversed in Theorem 2. That is, the stationary Gross–Pitaevskii equation (2) admits a unique Bloch wave solution *(5)* for $\varepsilon \in [0, \varepsilon_0)$ and three Bloch wave solutions for $\varepsilon \in (-\varepsilon_0, 0)$.

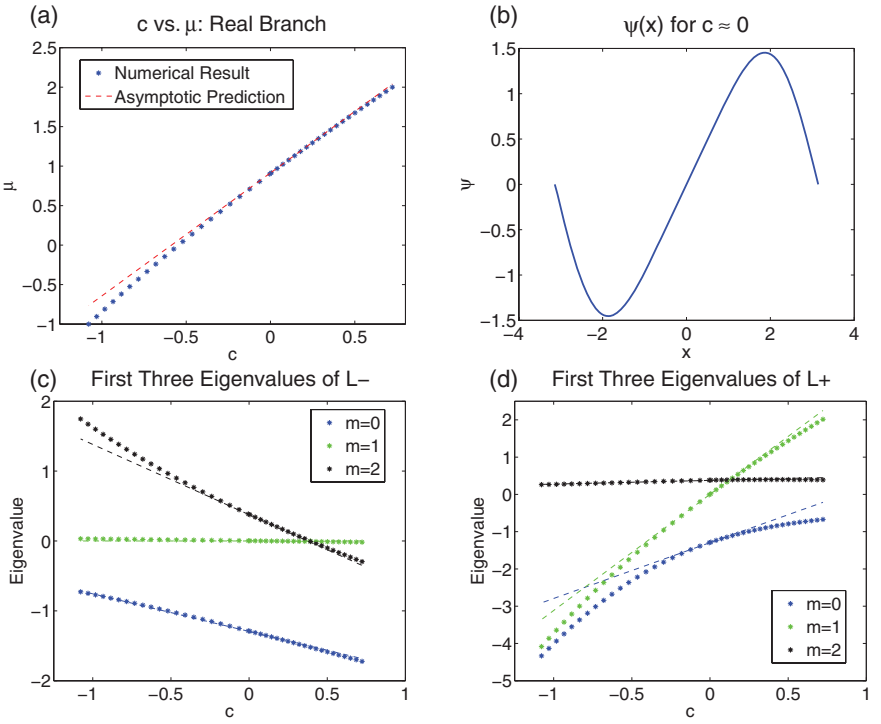

Figure 5. Similar to Figure 1 but with $k = 0$ and $n = 1$. Note the change in sign of the eigenvalue with $m = 2$ of $L_{-}(c)$ at $c \approx 0.4$.

4.1 Stationary normal form

In order to study loops in the Bloch energy band we must consider k slightly perturbed from $k = \frac{1}{2}$ and thus we take,

$$k = \frac{1}{2} + p, \tag{55}$$

for small p. If ψ is the Bloch wave (4) then we have,

$$\psi(x) = e^{ikx}\phi(x) = e^{ipx}e^{\frac{ix}{2}}\phi(x) \equiv e^{ipx}\widetilde{\psi}(x), \tag{56}$$

where $\phi(x + 2\pi) = \phi(x)$ and $\widetilde{\psi}(x + 2\pi) = -\widetilde{\psi}(x)$. As a result, we can reformulate the stationary equation (2) for the Bloch wave (56) in the form,

$$\begin{aligned} -\psi'' + V(x)\psi + c\psi^3 &= (\mu - p^2)\psi + 2ip\psi', \\ \psi(x + 2\pi) &= -\psi(x), \ \|\psi\|_{L^2} = 1, \end{aligned} \tag{57}$$

where the tilde sign is dropped for convenience.

Now we consider a neighbourhood of the bifurcation point and define,

$$c = c_* + \varepsilon, \qquad \mu = \mu_* + M + p^2, \tag{58}$$

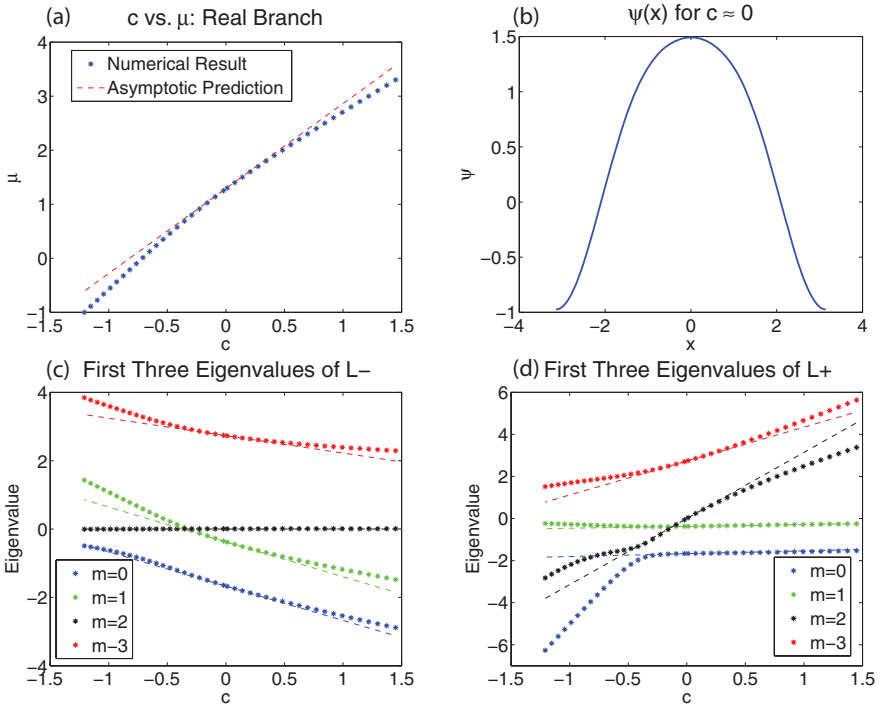

Figure 6. Similar to Figure 1 but with $k = 0$ and $n = 2$. Note the change in sign of the eigenvalue with $m = 1$ of $L_-(c)$ at $c \approx -0.3$.

where ε and M are small parameters. Parameters c and μ (and thus ε and M) are related along the stationary real branch that corresponds to $p = 0$. Let us decompose $\psi(x)$ into,

$$\psi(x) = \psi_*(x) + ia\varphi_*(x) + u(x) + iW(x), \quad \langle W, \varphi_* \rangle_{L^2} = 0, \tag{59}$$

with $u, W \in \mathcal{H}^2_{a.p.}$, and $a \in \mathbb{R}$. If we normalize $\|\psi_*\|_{L^2} = \|\varphi_*\|_{L^2} = 1$, then the normalization condition $\|\psi\|_{L^2} = 1$ gives,

$$0 = 2\langle \psi_*, u \rangle_{L^2} + \|u\|^2_{L^2} + a^2 + \|W\|^2_{L^2}. \tag{60}$$

Operator L_-^* has a two-dimensional kernel, $\mathrm{Ker}(L_-^*) = \{\psi_*, \varphi_*\}$. This motivates us to make the following decomposition, $L^2 = \{\psi_*, \varphi_*\} \oplus \mathrm{Ran}(L_-^*)$ where,

$$\mathrm{Ran}(L_-^*) = \{f \in L^2 : \quad \langle f, \psi_* \rangle_{L^2} = \langle f, \varphi_* \rangle_{L^2} = 0\}. \tag{61}$$

We again introduce the projection operator $P_- : L^2 \to \mathrm{Ran}(L_-^*)$ and state from standard methods that there exists $N_\pm > 0$ such that,

$$\|P_-(L_-^*)^{-1}P_-\|_{H^2 \to H^2} \leq N_-, \quad \|(L_+^*)^{-1}\|_{H^2 \to H^2} \leq N_+.$$

Substituting (59) into (57) and equating the real and imaginary parts yields,

$$(L_+^* + 3\varepsilon\psi_*^2 - M)u \;=\; H_+ + N_+(u, W) + K_+(W; p), \tag{62}$$

$$(L_-^* + \varepsilon\psi_*^2 - M)W \;=\; H_- + N_-(u, W) + K_-(u; p), \tag{63}$$

where,

$$\begin{aligned}
&H_+ := M\psi_* - \varepsilon\psi_*^3,\\
&N_+ := -(\varepsilon + c_*)((3u^2 + (a\varphi_* + W)^2)\psi_* + (u^2 + (a\varphi_* + W)^2)u),\\
&K_+ := -2p(a\varphi_*' + W'),\\
&H_- := Ma\varphi_* - \varepsilon a\psi_*^2\varphi_*,\\
&N_- := -(\varepsilon + c_*)(2\psi_* u + u^2 + (a\varphi_* + W)^2)(a\varphi_* + W),\\
&K_- := 2p(\psi_*' + u').
\end{aligned}$$

A further examination of u and W is in order. If each function ψ_*, φ_*, u, and W have definite parity, then H_+, N_+, and K_+ have the same parity as ψ_*, u, W', and φ_*' where as H_-, N_-, and K_- have the same parity as φ_*, W, u', and ψ_*'. In addition, $L_\pm$ preserves parity. Hence, a unique solution for u, if it exists, must have the same parity as ψ_*, φ_*', and W'. Similarly, if a unique solution for W exists then it must have the same parity as φ_*, ψ_*', and u'. Note that ψ_* and φ_* have opposite parities, which suggests that u and W should continue to have the same parity as ψ_* and φ_*, respectively.

To obtain the normal form for pitchfork bifurcation, we now expand u as following:

$$u = Mu_1 + \varepsilon u_2 + a^2 u_3 + apu_4 + U, \tag{64}$$

where,

$$\begin{aligned}
&u_1 := (L_+^*)^{-1}\psi_*, u_2 := -(L_+^*)^{-1}\psi_*^3,\\
&u_3 := -c_*(L_+^*)^{-1}\varphi_*^2\psi_*, u_4 := -2(L_+^*)^{-1}\varphi_*'.
\end{aligned}$$

The normalization condition (60) is further expanded as,

$$\begin{aligned}
0 =\,& 2M\langle\psi_*, u_1\rangle_{L^2} + 2\varepsilon\langle\psi_*, u_2\rangle_{L^2} + 2a^2\langle\psi_*, u_3\rangle_{L^2} + a^2\\
&+ 2ap\langle\psi_*, u_4\rangle_{L^2} + \mathcal{O}\big(\|U\|_{L^2}, \|W\|_{L^2}^2\big).
\end{aligned} \tag{65}$$

Assuming that $\langle\psi_*, u_1\rangle_{L^2} = \langle\psi_*, (L_+^*)^{-1}\psi_*\rangle_{L^2} \equiv S_0 \neq 0$, then there is a unique solution of the expansion (65) for M given by,

$$M = \alpha_0\varepsilon + \beta_0 a^2 + \gamma_0 ap + \mathcal{O}\big(\|U\|_{L^2}, \|W\|_{L^2}^2\big), \tag{66}$$

where,

$$\alpha_0 := -\frac{\langle\psi_*, u_2\rangle_{L^2}}{\langle\psi_*, u_1\rangle_{L^2}},\; \beta_0 := -\frac{1 + 2\langle\psi_*, u_3\rangle_{L^2}}{2\langle\psi_*, u_1\rangle_{L^2}},\; \gamma_0 := -\frac{\langle\psi_*, u_4\rangle_{L^2}}{\langle\psi_*, u_1\rangle_{L^2}}.$$

We see later that the $\mathcal{O}(ap)$ term is small enough to ignore. Using the nearly-identity transformation (64), we rewrite equation (62) in the following way,

$$U = (L_+^*)^{-1}(N_+ + c_* a^2 \varphi_*^2 \psi_* + Mu - 3\varepsilon \psi_*^2 u - 2pW') \equiv \mathcal{A}_+(U; W, \varepsilon, a, p). \tag{67}$$

Note that $M = M(\varepsilon, a^2, ap, \|U\|_{L^2}, \|W\|_{L^2}^2)$ follows from the expansion (66). The following lemma determines solutions of the fixed-point equation (67) for some given (W, ε, a, p).

LEMMA 4. *There exist $\varepsilon_0 > 0$, $p_0 > 0$, $a_0 > 0$, $\delta_0 > 0$, and $D > 0$ such that for all $|\varepsilon| < \varepsilon_0$, $|p| < p_0$, $|a| < a_0$, and $\|W\|_{H^2} < \delta$, the nonlinear operator $\mathcal{A}_+(U; W, \varepsilon, a, p) : \mathcal{H}^2_{a.p.} \to \mathcal{H}^2_{a.p.}$ has a unique fixed point in a neighbourhood of $0 \in \mathcal{H}^2_{a.p.}$ satisfying,*

$$\|U\|_{H^2} \le D\big(\varepsilon^2 + a^4 + a^2 p^2 + |a|\|W\|_{H^2}\big). \tag{68}$$

Proof: Again, we appeal to the Banach Fixed Point Theorem [20] by considering a neighbourhood of $0 \in \mathcal{H}^2_{a.p.}$,

$$\bar{\mathcal{B}}_r := \big\{U \in \mathcal{H}^2_{a.p.} : \|U\|_{H^2} \le r\big\}. \tag{69}$$

One can show, similarly to the proof of Lemma 2, that if $(W, \varepsilon, a, p) \in \mathcal{H}^2_{a.p.} \times \mathbb{R} \times \mathbb{R} \times \mathbb{R}$ are small then $\mathcal{A}_+$ maps $\bar{\mathcal{B}}_r$ into itself and that $\mathcal{A}_+$ is a contraction mapping. □

Now we consider equation (63) for W and after u is eliminated by expansion (64) with the bound (68). The corresponding equation is written as,

$$L_-^* W = (M - \varepsilon \psi_*^2) W + H_- + N_- + K_- \equiv \mathcal{G}(W; \varepsilon, a, p). \tag{70}$$

To have $\mathcal{G} \in \mathrm{Ran}(L_-^*)$ we set the constraints,

$$\langle \mathcal{G}, \varphi_* \rangle_{L^2} = 0, \quad \langle \mathcal{G}, \psi_* \rangle_{L^2} = 0, \tag{71}$$

since $\{\varphi_*, \psi_*\} = \mathrm{Ker}(L_-^*)$. Constraint $\langle \mathcal{G}, \psi_* \rangle_{L^2} = 0$ is satisfied trivially because ψ_* and $\mathcal{G}$ have opposite parities. By expanding constraint $\langle \mathcal{G}, \varphi_* \rangle_{L^2} = 0$ we obtain,

$$\begin{aligned} 0 = {} & Ma\big(1 - 2c_* \langle \psi_* \varphi_*^2, u_1 \rangle_{L^2}\big) - c_* a^3 \big(2\langle \psi_* \varphi_*^2, u_3 \rangle_{L^2} + \|\varphi_*\|_{L^4}^4\big) \\ & - \varepsilon a \big(\langle \psi_*^2, \varphi_*^2 \rangle_{L^2} + 2c_* \langle \psi_* \varphi_*^2, u_2 \rangle_{L^2}\big) + 2p \langle \psi_*', \varphi_* \rangle_{L^2} \\ & + \mathcal{O}(\varepsilon^2 a, a^5, p^2 a, p\varepsilon, a\|U\|_{L^2}, \varepsilon \|W\|_{L^2}), \end{aligned} \tag{72}$$

where $\|U\|_{L^2}$ is controlled by (68) and M is controlled by (66). As a result, we obtain a relationship between ε, a, p, and W:

$$\varepsilon a P_0 + a^3 Q_0 + p R_0 + \mathcal{O}(\varepsilon^2 a, a^5, \varepsilon \|W\|_{L^2}) = 0, \tag{73}$$

with,

$$P_0 := -\langle \psi_*^2, \varphi_*^2 \rangle_{L^2} - 2c_* \langle \psi_* \varphi_*^2, u_2 \rangle_{L^2} + \alpha_0 \big(1 - 2c_* \langle \psi_* \varphi_*^2, u_1 \rangle_{L^2}\big),$$
$$Q_0 := -c_* \big(2\langle \psi_* \varphi_*^2, u_3 \rangle_{L^2} + \|\varphi_*\|_{L^4}^4\big) + \beta_0 \big(1 - 2c_* \langle \psi_* \varphi_*^2, u_1 \rangle_{L^2}\big),$$
$$R_0 := 2\langle \psi_*', \varphi_* \rangle_{L^2}.$$

We say that the expansion (73) is the normal form for the pitchfork bifurcation at $c = c_*$. Note that equation (73) does not provide a unique solution for a. If p is as small as the other terms in (73), then $|p| = \mathcal{O}(a^3) = \mathcal{O}(a\varepsilon)$ and hence $|ap| = \mathcal{O}(a^4)$ is negligible in the expansion (66). Assuming that $R_0 \neq 0$, we can solve equation (73) uniquely for p and eliminate p from further computations.

Now we rewrite equation (70) as the fixed-point equation,

$$W = (P_-(L_-^*)^{-1} P_-)\mathcal{G} \equiv \mathcal{A}_-(W; \varepsilon, a), \tag{74}$$

where p is controlled by the expansion (73). The following lemma determines solutions of the fixed-point equation (74) for some given (ε, a).

LEMMA 5. *There exist $\varepsilon_0 > 0$, $a_0 > 0$, and $D > 0$, such that for all $|\varepsilon| < \varepsilon_0$ and $|a| < a_0$, the nonlinear operator $\mathcal{A}_-(W; \varepsilon, a) : \mathcal{H}^2_{a.p.} \to \mathcal{H}^2_{a.p.}$ has a unique fixed point in a neighbourhood $0 \in \mathcal{H}^2_{a.p.}$ satisfying,*

$$\|W\|_{H^2} \leq D(|\varepsilon a| + |a|^3). \tag{75}$$

Proof: The proof is similar to the proofs of Lemma 2 and Lemma 4. □

We are now equipped to prove Theorem 2. Expansion (66) tells us that the number of branches for μ, as in (58), will depend on the number of admissible values for a in the normal form (73). For $p = 0$, the assumption of $\text{sign}(P_0 Q_0) = -1$ implies that equation (73) admits only one solution $a = 0$ if $\varepsilon \leq 0$ and three solutions $a = 0$ and $a = \pm\sqrt{-P_0/Q_0}\varepsilon^{1/2} + \mathcal{O}(\varepsilon^{3/2})$ for $\varepsilon > 0$.

Now consider $p \neq 0$ but small. Note that the p^2 term in (58) is negligible since $|p| = \mathcal{O}(a^3)$. For a small ε, the discriminant of the perturbed cubic equation (73) is given by,

$$\Delta(p, \varepsilon) := -4Q_0(\varepsilon P_0)^3 - 27(Q_0 p P_0)^2 + \mathcal{O}(\varepsilon^4). \tag{76}$$

Because $\text{sign}(P_0 Q_0) = -1$, we have $\Delta < 0$ for small $\varepsilon \leq 0$. This is the condition required for the normal form (73) to admit one (real) solution in a. For small $\varepsilon > 0$, we define $p = p_0(\varepsilon)$ from the zero of $\Delta(p, \varepsilon)$,

$$p_0(\varepsilon) := \sqrt{\frac{-4P_0}{27Q_0}}\varepsilon^{3/2} + \mathcal{O}(\varepsilon^{5/2}). \tag{77}$$

For any $|p| < p_0(\varepsilon)$ and small $\varepsilon > 0$, the normal form (73) admits three solutions for a. These solutions correspond to three different Bloch waves. The proof of Theorem 2 appears to be complete.

We remark that the arguments in the proof of Theorem 2 could be repeated around $k = 0$ simply by changing the boundary condition in the stationary system (57) to $\psi(x + 2\pi) = \psi(x)$ and working with $\psi \in \mathcal{H}^2_p$. Such a configuration occurs on Figure 5, which satisfies the conditions for bifurcation of the stationary real branch for $c_* > 0$.

As for $c_* < 0$ as in the configuration on Figure 6, the analysis can be repeated as in Theorem 2 with $c = c_* + \varepsilon$ and $\mu = \mu_* + M$ so that a loop in the Bloch band will appear when $\varepsilon < 0$ but now under the assumption $\text{sign}(P_0 Q_0) = +1$.

The side of ε, either $\varepsilon > 0$ or $\varepsilon < 0$, for which we have one or three Bloch wave solutions near $k = 0$ or $k = \frac{1}{2}$ depends on the sign of $P_0 Q_0$. We evaluate this sign numerically and do in fact see the correct orientation of the solution branches.

Before numerical computations, we note that the sign of P_0 is determined by the motion of the eigenvalue of $L_-(c)$ that crosses zero at $c = c_*$.

LEMMA 6. *Let P_0 be defined by (73) and $\lambda_-^{(n)}(c)$ be the nth eigenvalue of L_- such that $\lambda_-^{(n)}(c_*) = 0$ and the corresponding eigenfunction at $c = c_*$ is φ_*. Then,*

$$\lambda_-^{(n)\prime}(c_*) = -P_0. \tag{78}$$

Proof: We set $p = 0$ and $a = 0$ in the previous computations, in particular we set,

$$c = c_* + \varepsilon, \quad \mu = \mu_* + M, \tag{79}$$

and,

$$\psi = \psi_* + M u_1 + \varepsilon u_2 + \mathcal{O}(\varepsilon^2 + M^2), \tag{80}$$

with u_1 and u_2 defined by (64). Substituting (80) to the operator $L_-(c)$ yields,

$$L_-(c) = L_-^* + \varepsilon \psi_*^2 + 2c_*(\psi_* M u_1 + \psi_* \varepsilon u_2) - M + \mathcal{O}(\varepsilon^2 + M^2). \tag{81}$$

The Rayleigh quotient (40) now gives us,

$$\begin{aligned} \lambda_-^{(n)}(c) &= \left\langle L_-(c)\varphi_-^{(n)}, \varphi_-^{(n)} \right\rangle_{L^2} \\ &= \varepsilon \left\langle \psi_*^2, \varphi_*^2 \right\rangle_{L^2} + 2c_* M \left\langle \psi_* \varphi_*^2, u_1 \right\rangle_{L^2} - M \\ &\quad + 2c_* \varepsilon \left\langle \psi_* \varphi_*^2, u_2 \right\rangle_{L^2} + \mathcal{O}(\varepsilon^2 + M^2), \end{aligned}$$

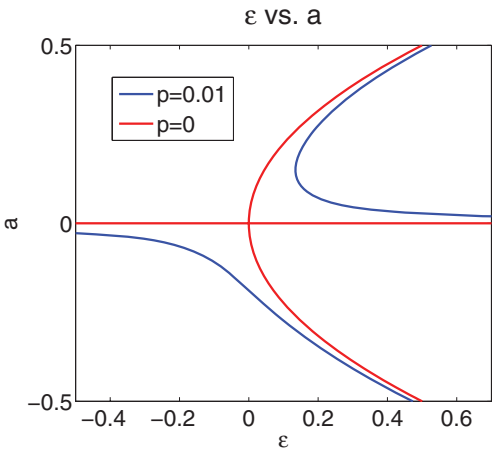

Figure 7. The dependence of a versus ε for $n = 0$ and two values of $p = k - \frac{1}{2}$. When $p = 0$, a pitchfork bifurcation is observed. When $p > 0$, the symmetry is broken and the unfolded pitchfork bifurcation is observed.

once we note that $L_-^* \varphi_* = 0$. If $M = \alpha_0 \varepsilon + \mathcal{O}(\varepsilon^2)$ then,

$$\begin{aligned} \lambda_-^{(n)\prime}(c_*) = &\left\langle \psi_*^2, \varphi_*^2 \right\rangle_{L^2} + \alpha_0 \left(2c_* \left\langle \psi_* \varphi_*^2, u_1 \right\rangle_{L^2} - 1 \right) \\ &+ 2c_* \left\langle \psi_* \varphi_*^2, u_2 \right\rangle_{L^2} = -P_0, \end{aligned} \tag{82}$$

which is the desired result. □

COROLLARY 2. *If $\lambda_-^{(n)\prime}(c_*) < 0$, that is, the eigenvalue $\lambda_-^{(n)}(c)$ crosses 0 from positive to negative values as c increases, then $P_0 > 0$.*

If Corollary 2 is applied, condition $\operatorname{sign}(P_0 Q_0) = -1$ of Theorem 2 is satisfied if $Q_0 < 0$.

4.2 Examples of loop bifurcations

We now illustrate the results of Theorem 2 using the simplest examples.

4.2.1. Example with $k = \frac{1}{2}$, $n = 0$ and $c_* > 0$ (Figure 1). If $V(x) = \cos(x)$, then there exists an analytical solution for the bifurcation [17] with $c_* = 1$, $\mu_* = \frac{5}{4}$,

$$\psi_*(x) = \sqrt{2} \sin\left(\frac{x}{2}\right), \qquad \varphi_*(x) = \sqrt{2} \cos\left(\frac{x}{2}\right). \tag{83}$$

We evaluate coefficients S_0, P_0, Q_0, R_0 numerically,

$$S_0 \approx 0.3647, \quad P_0 \approx 0.7419, \quad Q_0 \approx -1.4838, \quad R_0 = -1.$$

We can now solve the normal form (73) for a in terms of ε for a fixed value of p. A plot with $p = 0$ and small $p > 0$ is shown in Figure 7. Once we solve for

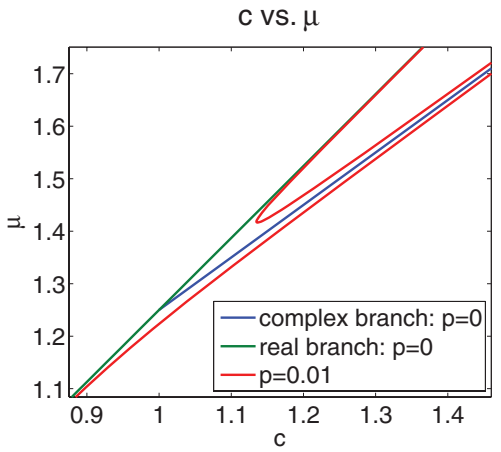

Figure 8. The dependence of μ versus c for $n = 0$ and two values of $p = k - \frac{1}{2}$. For $p = 0$, we see the stationary real branch (green), as seen numerically in Figure 1. The new (complex) solution is observed below the real branch for $c > c_* = 1$. The red curve gives solutions branches for $p \neq 0$. One solution branch is seen for $c < c_+(p)$, where $c_+(p) > c_*$. Three solution branches are observed for $c > c_+(p) > c_*$.

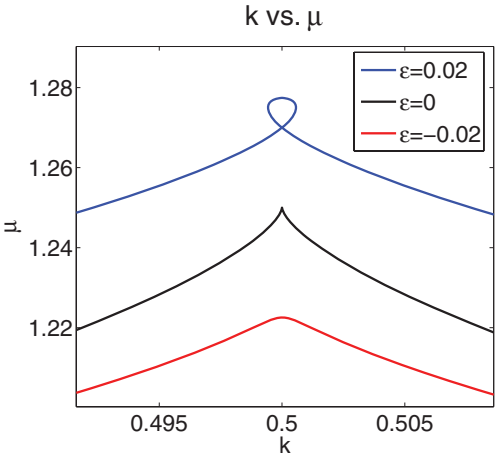

Figure 9. The dependence of μ versus k for $n = 0$ and three values of $c = c_* + \varepsilon$. The transition of the Bloch band through the bifurcation is seen. For $c < c_*$, the curve is smooth. At $c = c_*$, a cusp point forms. Above the bifurcation value $c > c_*$, a loop forms in the energy band.

a in terms of ε we can solve for M in terms of ε in (66). Using (58), we plot solution branches on the (c, μ) diagram in Figure 8. Because we have found the relationship between M and ε we can now solve for M as a function of p in (73) and so μ as a function of k from (58) and (55). In this way Figure 9 shows the Bloch bands around $k = \frac{1}{2}$ for values of c close to c_* (small ε).

Let us define,

$$c_+(p) = c_* + \varepsilon_{+(p)}, \tag{84}$$

where, according to (77),

$$\varepsilon_{+(p)} = \sqrt[3]{\frac{-27Q_0}{4P_0}p^{2/3} + \mathcal{O}(p^{4/3})}. \tag{85}$$

For small p and $c > c_+(p)$, three solution branches exist according to Theorem 2.

In Figure 7, we see clearly the pitchfork bifurcation of the stationary real branch. Parameter a here represents the magnitude of the imaginary component of ψ. For $p = 0$, red in Figure 7, and $\varepsilon < 0$ we see the only solution has $a = 0$ and so is purely real. For $\varepsilon > 0$, we see the persistence of the real solution ($a = 0$) and the appearance of two new solution branches with $a \neq 0$. However, the values of a are equal in magnitude and so they represent complex-conjugate solutions with the same eigenvalue, μ. For $p \neq 0$, solutions cannot be purely real. One solution branch exists for $\varepsilon < \varepsilon_+(p)$ and three solution branches exist for $\varepsilon > \varepsilon_+(p)$.

In Figure 8 a similar behavior is observed. For $p = 0$, the stationary real branch persists for $c > c_*$ and the new (complex) branch bifurcates below the real branch for $c > c_*$. For $p \neq 0$, there is one solution branch for $c < c_+(p)$ and three solution branches for $c > c_+(p)$.

Now on to Figure 9. With $c < c_*$ we have a single solution for each k close to $k = \frac{1}{2}$. At $c = c_*$ the band forms a cusp at $k = \frac{1}{2}$ after which, $c > c_*$, we see the appearance of a loop. To show that $k = \frac{1}{2}$ is a cusp point for the band at $c = c_*$ ($\varepsilon = 0$), we note from (58), (66), and (73) that,

$$\left.\frac{d\mu}{dk}\right|_{k=\frac{1}{2}} = \left.\frac{dM}{dp}\right|_{p=0} = 2\beta_0 a \left.\frac{da}{dp}\right|_{p=0} = \frac{2\beta_0}{3}\left(\frac{R_0}{Q_0}\right)^{\frac{2}{3}} \left.\frac{1}{p^{\frac{1}{3}}}\right|_{p=0} = \infty. \tag{86}$$

The solution at the top of the loop on Figure 9 corresponds to the real branch. The complex-conjugate solutions are located at the bottom of the loop, where the loop intersects itself. The degeneracy stems from the two solutions having the same magnitude of a in Figure 7.

4.2.2. Example with $k = 0$, $n = 1$, and $c_* > 0$ (Figure 5). For this configuration, there is no closed form solution for c_*, μ_*, ψ_*, or φ_*. We must therefore approximate these values and functions numerically. We implement a root finding scheme on the third eigenvalue of L_- ($m = 2$ in Figure 5) to find the value $c = c_*$, where this eigenvalue crosses zero. Numerically we compute $c_* \approx 0.3942$ and $\mu_* \approx 1.5154$. Then, ψ_* and φ_* are given as the eigenfunctions of the two zero eigenvalues of L_- at $c = c_*$. Once we approximate ψ_* and φ_*

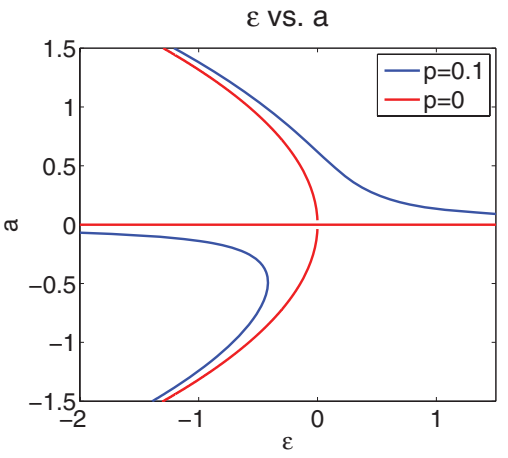

Figure 10. The dependence of a versus ε for $n = 2$ and two values of $p = k$. Behavior is similar to Figure 7 but the orientation is reversed.

numerically we can compute the normal form coefficients,

$$S_0 \approx 0.8602, \quad P_0 \approx 0.8996, \quad Q_0 \approx -0.7871, \quad R_0 \approx -1.7567.$$

As a result, we obtain $\text{sign}(P_0 Q_0) = -1$ as desired.

The bifurcation diagram, the solution branches around the bifurcation point $c = c_*$, and the Bloch bands are qualitatively similar to Figures 7–9.

4.2.3. Example with $k = 0$, $n = 2$, and $c_* < 0$ (Figure 6). For this configuration, we compute numerically, $c_* \approx -0.3253$ and $\mu_* \approx 0.7521$. When the values of c are reduced, it is the second eigenvalue of L_- that crosses zero ($m = 1$ in Figure 6). Normal form coefficients are found to be,

$$S_0 \approx -0.8685, \quad P_0 \approx 1.3158, \quad Q_0 \approx 0.7829, \quad R_0 \approx 1.8295.$$

We obtain $\text{sign}(P_0 Q_0) = +1$, which gives three solution branches for $\varepsilon < 0$ or $c < c_* < 0$. Figures 10, 11, and 12 characterize the relevant bifurcation similar to Figures 7, 8, and 12. The only difference is that the loop appears upside down in the case $c_* < 0$.

5. Stability of Bloch waves at the lowest energy band

When a pitchfork (symmetry-breaking) bifurcation occurs, it is important to classify stability of different branches of stationary solutions. We study stability of the three branches in the loop using the time-dependent analogue of the Lyapunov–Schmidt reduction method. In particular, we will derive the

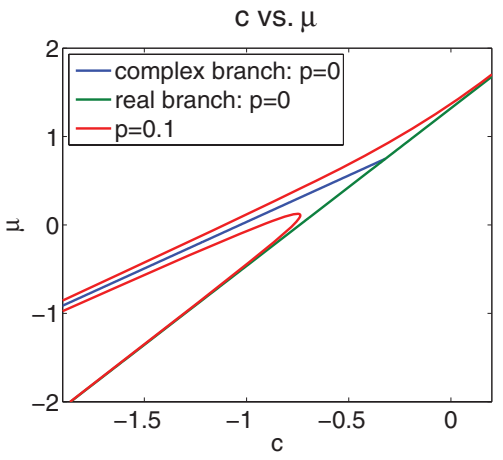

Figure 11. The dependence of μ versus c for $n = 2$ and two values of $p = k$. Behaviour is similar to Figure 8 but the orientation is reversed.

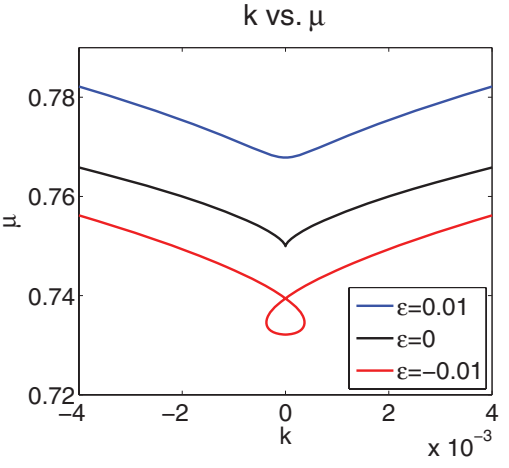

Figure 12. The dependence of μ versus k for $n = 2$ and three values of $c = c_* + \varepsilon$. For $c > c_*$, the curve is smooth. At the bifurcation value $c = c_*$, a cusp forms. When $c < c_*$, a loop forms in the energy band.

time-dependent normal form for the pitchfork bifurcation in Section 5.1. Details of the Lyapunov–Schmidt reduction method in a similar context of the pitchfork bifurcation of stationary localized states in double-well potentials can be found in [5, 12].

Section 5.2 reports a rigorous result on the stability of the stationary Bloch waves associated with the lowest energy band. Section 5.3 confirms the results with direct numerical simulations of the Gross–Pitaevskii equation (1).

5.1. Time-dependent normal form

We set again $c = c_* + \varepsilon$ and $k = \frac{1}{2} + p$, for small ε and p. A solution of the Gross–Pitaevskii equation (1) is now decomposed as follows:

$$\Psi(x,t) = e^{-i\mu_* t - i\int_0^t M(\tau)d\tau}(\psi_*(x) + i a(t)\,\varphi_*(x) + u(x,t) + i\,W(x,t)). \tag{87}$$

Decomposition into the real and imaginary parts gives the evolution equations for u and W,

$$W_t + (L_+^* + 3\varepsilon\psi_*^2 - M)u = -\dot{a}\varphi_* + H_+ + N_+(u,W) + K_+(W;p), \tag{88}$$

$$-u_t + (L_-^* + \varepsilon\psi_*^2 - M)W = H_- + N_-(u,W) + K_-(u;p), \tag{89}$$

where $H_\pm$, $N_\pm$, and $K_\pm$ are defined below system (62)–(63). We decompose u similarly to the stationary decomposition (64) but with one additional term,

$$u = Mu_1 + \varepsilon u_2 + a^2 u_3 + apu_4 + \dot{a}u_5 + U, \tag{90}$$

where,

$$u_5 := -(L_+^*)^{-1}\varphi_*.$$

The normalization condition, $\|\Psi(\cdot,t)\|_{L^2} = 1$, now reads,

$$\begin{aligned} 0 = {} & 2M\langle\psi_*, u_1\rangle_{L^2} + 2\varepsilon\langle\psi_*, u_2\rangle_{L^2} + 2a^2\langle\psi_*, u_3\rangle_{L^2} \\ & + a^2 + 2ap\langle\psi_*, u_4\rangle_{L^2} + \mathcal{O}\left(\|U\|_{L^2}, \|W\|_{L^2}^2\right), \end{aligned} \tag{91}$$

where $\langle\psi_*, u_5\rangle_{L^2} = -\langle\psi_*, (L_+^*)^{-1}\varphi_*\rangle_{L^2} = 0$, thanks to the opposite parity of ψ_* and φ_*. The normalization condition (91) gives the same expression for M as in (66),

$$M = \alpha_0\varepsilon + \beta_0 a^2 + \mathcal{O}\big(|ap|, \|U\|_{L^2}, \|W\|_{L^2}^2\big), \tag{92}$$

but a and M are now time-dependent. Equation (89) for W now reads,

$$L_-^* W = \mathcal{G}(\varepsilon, a, p, W) + \dot{M}u_1 + 2a\dot{a}u_3 + \dot{a}pu_4 + \ddot{a}u_5 + U_t \equiv \mathcal{E}, \tag{93}$$

where $\mathcal{G}$ is as defined in (70). In order to have $\mathcal{E} \in \mathrm{Ran}(L_-^*)$ we require,

$$\frac{d}{dt}\langle\psi_*, u\rangle_{L^2} = -\langle\psi_*, \mathcal{G}\rangle_{L^2}, \tag{94}$$

$$\frac{d}{dt}\langle\varphi_*, u\rangle_{L^2} = -\langle\varphi_*, \mathcal{G}\rangle_{L^2}. \tag{95}$$

The first constraint (94) is already satisfied because the normalization condition, $\|\Psi(\cdot,t)\|_{L^2} = 1$. The second constraint (95) gives,

$$\ddot{a}\langle\varphi_*, u_5\rangle_{L^2} + \langle\varphi_*, \mathcal{G}\rangle_{L^2} = -\frac{d}{dt}\langle\varphi_*, U\rangle_{L^2}, \tag{96}$$

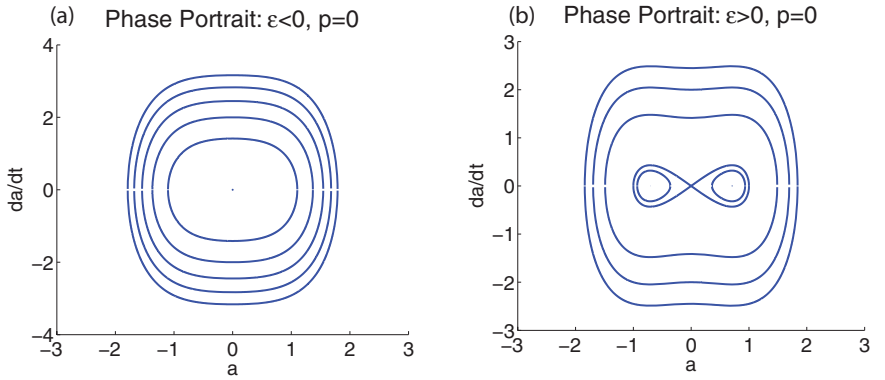

Figure 13. Phase portraits for $p = 0$. (a) $\varepsilon < 0$: one equilibrium; center. (b) $\varepsilon > 0$: three equilibria; two centers and one saddle.

where we have used that $\langle \varphi_*, u_1 \rangle_{L^2} = \langle \varphi_*, u_3 \rangle_{L^2} = \langle \varphi_*, u_4 \rangle_{L^2} = 0$. Expanding at the highest order yields the time-dependent normal form equation,

$$\ddot{a} N_0 + \varepsilon a P_0 + a^3 Q_0 + p R_0 + \mathcal{O}(\varepsilon^2 a, a^5, a\|U\|_{L^2}, \varepsilon\|W\|_{L^2}, \|U_t\|_{L^2}) = 0, \tag{97}$$

where P_0, Q_0, and R_0 are as in the stationary normal form (73) and,

$$N_0 := \langle \varphi_*, u_5 \rangle_{L^2} = -\left\langle \varphi_*, (L_+^*)^{-1} \varphi_* \right\rangle_{L^2}.$$

The justification of the time-dependent normal form (97) hinges on the smallness of $a\|U\|_{L^2}$, $\varepsilon\|W\|_{L^2}$, and $\|U_t\|_{L^2}$, the proof of which is similar to the analysis in [12].

Phase portraits for the truncated normal form equation (97) can be obtained by plotting the level curves of the energy equation,

$$E = \frac{\dot{a}^2 N_0}{2} + \frac{\varepsilon a^2 P_0}{2} + \frac{a^4 Q_0}{4} + paR_0, \tag{98}$$

for various values of E. Note that $N_0 < 0$ if $(L_+^*)^{-1}$ is positive definite (as for the lowest energy band, $n = 0$). Indeed, for the example with $n = 0$, $k = \frac{1}{2}$, and $c_* > 0$ (Section 4.2.1) we find the numerical value $N_0 \approx -1.3480$.

Phase portraits for $p = 0$ are seen in Figure 13. If $\varepsilon < 0$, we see that the only equilibrium point at (0, 0) is a stable center point. If $\varepsilon > 0$, three equilibrium points are present. The solution with $a = 0$ is a saddle point and therefore unstable. The two other solutions are centers and so stable. Figure 14 shows phase portraits for small $p \neq 0$. If $p \neq 0$, we see similar dynamics even though the symmetry of the problem is broken.

Figures 13 and 14 illustrate a typical behavior of a supercritical pitchfork bifurcation. The stationary real branch is stable before the bifurcation but loses its stability after the bifurcation as the stable complex-conjugate solutions

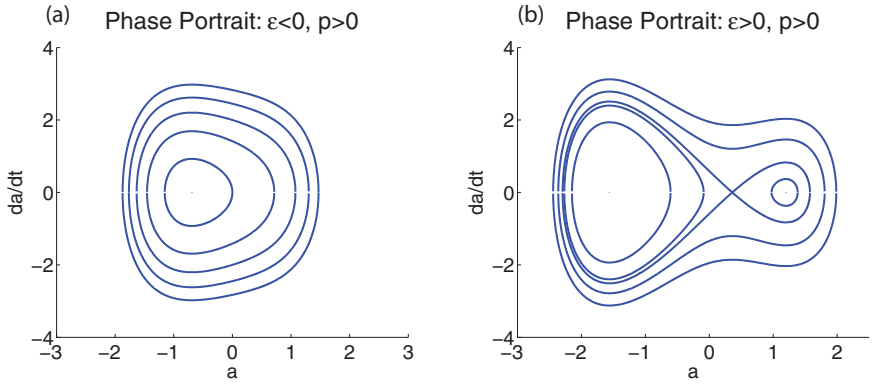

Figure 14. Phase portraits for $p \neq 0$. (a) $\varepsilon < 0$: one equilibrium; center. (b) $\varepsilon > 0$: three equilibria; two centers and one saddle.

appear. Away from $k = \frac{1}{2}$, the single branch which exists for $c < c_*$ is stable and remains stable for $c > c_*$. Of the two new branches that appear for $c > c_*$, as a result of the saddle-node bifurcation, one is stable and the other is unstable. In Figure 7 the branch with the smallest $|a|$ is the unstable branch. This corresponds to the branch in Figure 8 with the largest value for μ. So in Figure 9 the top of the loop is unstable while the bottom of the loop and branch leading up to the loop are stable.

For the example with $n = 1$, $k = 0$, and $c_* > 0$ (Section 4.2.2), we numerically compute $N_0 \approx -2.4725 < 0$. Hence, phase portraits for this configuration will be qualitatively the same as Figures 13 and 14 and so the stability of the stationary branches will be identical to the case when $n = 0$, $k = \frac{1}{2}$, and $c_* > 0$.

For the example with $n = 2$, $k = 0$, and $c_* < 0$ (Section 4.2.3), we find numerically $N_0 \approx 2.5149$. The reversed signs of $N_0 > 0$ and $\text{sign}(P_0 Q_0) = +1$ gives behavior similar to Figures 13 and 14. The exchange of stability between the solution branches therefore remains the same.

5.2 Spectral stability of the lowest energy band

We prove rigorously that the stationary real branch at $k = \frac{1}{2}$ is spectrally stable up to the bifurcation point $c < c_*$ and becomes unstable for $c > c_*$ under the assumption that the second eigenvalue of operator $L_-(c)$ crosses zero from positive to negative values at $c = c_*$. This assumption is justified for the lowest energy band (Figure 1). Recall that the first eigenvalue of $L_-(c)$ is located at 0 for any $c \in \mathbb{R}$.

Spectral stability of the real stationary branch is determined by the eigenvalues of the linearized system,

$$L_+(c)U = -\lambda W, \quad L_-(c)W = \lambda U, \tag{99}$$

where operators $L_{\pm}(c)$ are given by (18)–(19), and $(U, W) \in \mathcal{H}^2_{a.p.} \times \mathcal{H}^2_{a.p.}$. If there is an eigenvalue with $\mathrm{Re}(\lambda) > 0$, the stationary real solution $\psi \in \mathcal{H}^2_{a.p.}$ is unstable with respect to antiperiodic perturbations (U, W). Otherwise, it is spectrally stable. The following lemma clarifies the stability of the stationary real branch at the lowest energy band.

LEMMA 7. *Assume that the second eigenvalue of operator $L_-(c)$ at the stationary real branch is positive for $c < c_*$ and negative for $c > c_*$, whereas the first eigenvalue of $L_+(c)$ is negative for $c < 0$ and positive for $c > 0$. Then, the stationary real branch is stable for $c < c_*$ and unstable for $c > c_*$.*

Proof: Since $L_+(c)$ is positive for any $c > 0$ by the assumption, we can rewrite the eigenvalue problem (99) as the generalized eigenvalue problem [2, 10],

$$L_-(c)W = \gamma L_+^{-1}(c)W, \quad \gamma = -\lambda^2. \tag{100}$$

If $c \in (0, c_*)$, then operator $L_-(c)$ is nonnegative and $\gamma \geq 0$ ($\lambda \in i\mathbb{R}$) for any eigenvalue of the generalized eigenvalue problem (100). In this case, the stationary real solution is spectrally stable.

If $c > c_*$, operator $L_-(c)$ admits exactly one negative eigenvalue. By Sylvester's Inertia Law for linear operators [10], there is one negative eigenvalue of the generalized eigenvalue problem (100), which corresponds to an eigenvalue $\lambda \in \mathbb{R}_+$. In this case, the stationary real solution is spectrally unstable.

It remains to prove the stability of the stationary real branch for $c < 0$, when $L_+(c)$ has one negative eigenvalue and $L_-(c)$ is nonnegative. For this case, we introduce the constrained subspace of $\mathcal{H}^2_{a.p.}$, where $L_-(c)$ is strictly positive. Since $L_-(c)\psi = 0$ we define,

$$X_c = \left\{ U \in \mathcal{H}^2_{a.p.} : \quad \langle \psi, U \rangle_{L^2} = 0 \right\}.$$

If $U \in X_c$ and $\lambda \neq 0$, we can invert $L_-(c)$ on U and reduce the eigenvalue problem (99) to another generalized eigenvalue problem,

$$L_+(c)U = \gamma L_-^{-1}(c)U, \quad \gamma = -\lambda^2. \tag{101}$$

As is well known [10], the operator $L_+(c)|_{X_c}$ constrained on X_c is nonnegative if $\langle \psi, L_+^{-1}(c)\psi \rangle_{L^2} \leq 0$. From exact computations, it follows that $L_+^{-1}(c)\psi = \partial_\mu \psi$ hence,

$$\langle \psi, L_+^{-1}(c)\psi \rangle_{L^2} = \frac{1}{2}\frac{d}{d\mu}\|\psi\|^2_{L^2} = 0,$$

because of the normalization condition $\|\psi\|^2_{L^2} = 1$. Therefore, operator $L_+(c)|_{X_c}$ is nonnegative for any $c < 0$ and $\gamma \geq 0$ ($\lambda \in i\mathbb{R}$) for any eigenvalue of the generalized eigenvalue problem (101). In this case, the stationary real solution is spectrally stable. □

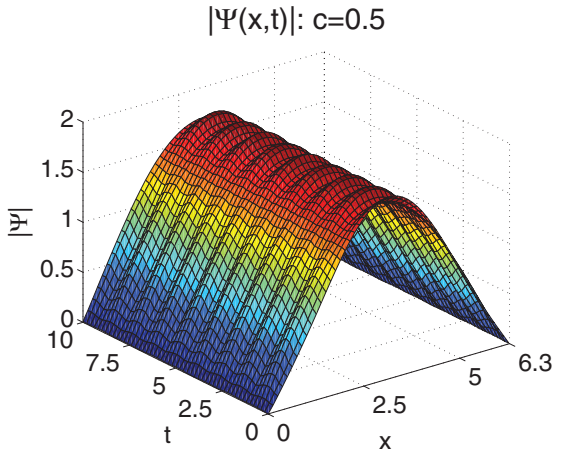

Figure 15. Time evolution of $|\Psi(x, t)|$ with $c = 0.5 < c_*$ and initial condition $\Psi(x, 0) = \chi\psi(x)$ for $k = \frac{1}{2}$ and $n = 0$. The oscillatory behavior indicates that the real stationary state ψ is stable.

We note that the stationary real branch at other energy bands correspond to operators $L_{\pm}(c)$ with several negative eigenvalues. As a result, the count of negative eigenvalues becomes less explicit [2] and instabilities of the corresponding real solutions may arise before the loop bifurcation in the parameter continuation in $c \in \mathbb{R}$.

5.3 Numerical simulations of the Gross–Pitaevskii equation

We now illustrate the stability of the stationary real branch at $k = \frac{1}{2}$ with some numerical simulations of the time-dependent Gross–Pitaevskii equation (1). The time-dependent solutions $\Psi(x, t)$ are approximated using the split-step Fourier method, where the initial condition $\Psi(x, 0)$ is chosen to be close to the stationary state of the lowest energy band.

In Figure 15, we take $c = 0.5 < c_*$ and $\Psi(x, 0) = \chi\psi(x)$, where $\chi \in \mathbb{R}$ is close to 1 and $\psi(x)$ is the real stationary solution for $k = \frac{1}{2}$ and $n = 0$. The solution surface $|\Psi(x, t)|$ shows stable oscillations near the real stationary state.

Figure 16 shows the solution surface $|\Psi(x, t)|$ for $c = 1.5 > c_*$ subject to the same initial condition $\Psi(x, 0) = \chi\psi(x)$. In this case a different dynamical pattern is observed. The solution $\Psi(x, t)$ does not remain close to the real stationary state $\psi(x)$ and instead oscillates about the complex stationary state.

Figures 17 and 18 illustrate the instability of the real stationary state and the stability of the complex stationary state. Figure 17 shows $\Psi(x, t)$ for two time instances $0 < t_1 < t_2$. At t_1 (which is close to $t = 0$), $\Psi(x, t_1)$ is close to the real stationary state, however, after some time we see that $\Psi(x, t_2)$ is far from the real stationary state but close to the complex stationary state. This behavior repeats as the solution $\Psi(x, t)$ oscillates about the complex stationary state.

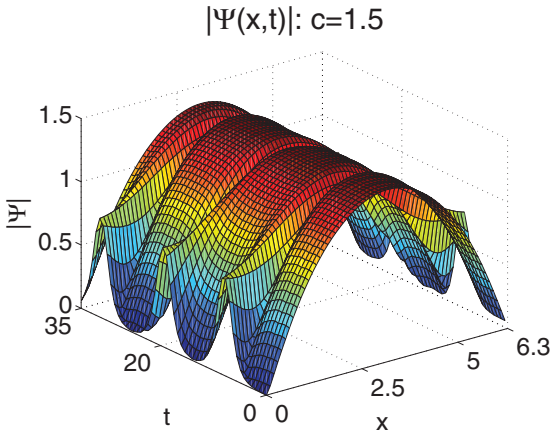

Figure 16. Time evolution of $|\Psi(x, t)|$ with $c = 1.5 > c_*$ and initial condition $\Psi(x, 0) = \chi\psi(x)$. The instability of the real stationary state ψ is observed.

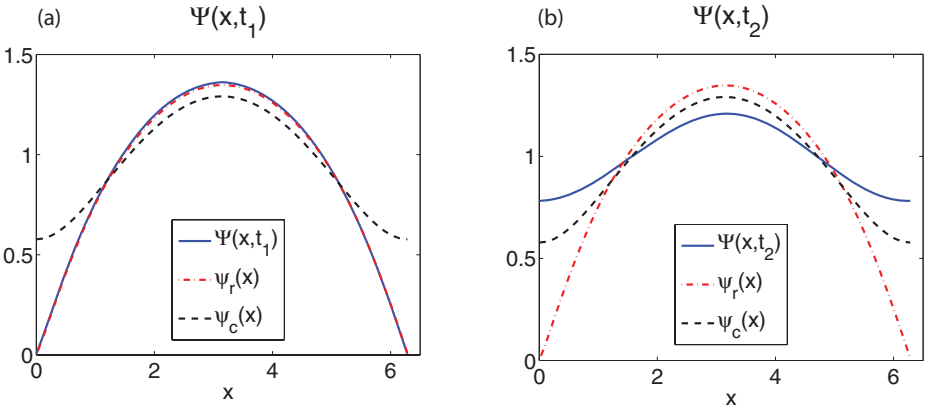

Figure 17. Plots of $\Psi(x, t)$ for two time instances superimposed on the real and complex stationary states for $c = 1.5$ as in Figure 16.

The periodic oscillations of $\Psi(0, t)$ on Figure 18 further indicates that the real stationary states has lost its stability and the complex stationary state is stable.

6. Comparison with Bloch waves in optical resonators

We discuss here the loop bifurcations in the context of atomic Bloch oscillations in optical cavities [14, 15]. A mathematical model for the coupled atom-cavity dynamics in a driven Fabry-Perot resonators is given by the linear Schrödinger

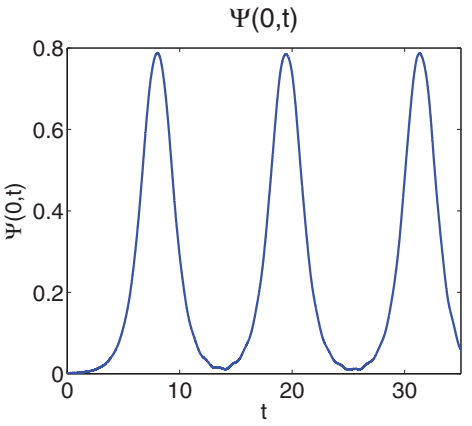

Figure 18. Periodic oscillations of $\Psi(0, t)$ for $c = 1.5$.

equations with a periodic potential,

$$i\frac{\partial \Psi}{\partial t} = \left(-\frac{\partial^2}{\partial x^2} + |\alpha|^2 \cos^2\left(\frac{x}{2}\right)\right)\Psi, \tag{102}$$

and the Heisenberg equation of motion,

$$\frac{d\alpha}{dt} = \left(i\Delta - iN\int_{-\pi}^{\pi} |\Psi(x,t)|^2 \cos^2\left(\frac{x}{2}\right) dx - K\right)\alpha + Q, \tag{103}$$

where $\Psi(x,t) : \mathbb{R} \times \mathbb{R} \to \mathbb{C}$ is the wave function occupied by all N atoms, $\alpha(t) : \mathbb{R} \to \mathbb{C}$ is the expectation value for the death operator (related to annihilation of a photon in the cavity field), and (N, Q, K, Δ) are positive constants.

Stationary states satisfy the stationary Schrödinger equation,

$$-\psi''(x) + |\alpha|^2 \cos^2\left(\frac{x}{2}\right)\psi(x) = \mu\psi(x), \tag{104}$$

where

$$\alpha = \frac{Q}{K - i\Delta + iN\int_{-\pi}^{\pi} |\psi(x)|^2 \cos^2\left(\frac{x}{2}\right) dx}.$$

The nonlinearity arises in an integral form through the variable α.

Loop bifurcations of energy bands were reported in [15] based on numerical approximations. We prove here that these loop bifurcations have a different nature from those in the optical lattices governed by the stationary Schrödinger equation (2) with the cubic nonlinearity. In particular, a change in the number of negative eigenvalues in the operator L_- for the stationary real branch is impossible in the continuations with respect to parameters (N, Q, K, Δ).

Let ψ_η be the Bloch wave of the linear Schrödinger equations,

$$-\psi''(x) + \eta \cos^2\left(\frac{x}{2}\right)\psi(x) = \mu\psi(x), \quad \eta > 0, \tag{105}$$

where μ depends on the Bloch wave number $k \in [-\frac{1}{2}, \frac{1}{2}]$ and the parameter η. The number of stationary Bloch waves for each $k \in [-\frac{1}{2}, \frac{1}{2}]$ is found from the implicit equation,

$$\eta = F(\eta; N, Q, K, \Delta) := \frac{Q^2}{K^2 + \left(\Delta - N\int_{-\pi}^{\pi} |\psi_\eta(x)|^2 \cos^2\left(\frac{x}{2}\right) dx\right)^2}. \tag{106}$$

For $k = 0$ and $k = \pm\frac{1}{2}$, the stationary Bloch wave ψ is real and the eigenvalues μ of the linear Schrödinger equations (105) are known to be simple for any $\eta > 0$ for lower-order energy bands (see Figure 6.1 in [18]).

In what follows, we consider ψ to be the real stationary branch for $k = 0$ or $k = \pm\frac{1}{2}$. Differentiating (104) with respect to imaginary ψ gives us operator,

$$L_- = -\partial_x^2 + \eta \cos^2\left(\frac{x}{2}\right) - \mu,$$

whereas differentiating (104) with respect to real ψ gives a complicated nonlocal expression for operator L_+. For any $\eta > 0$, operator L_- has a simple zero eigenvalue with the eigenfunction ψ_η and the zero eigenvalue remains simple in parameter continuations in $\eta > 0$. Hence, no complex solutions of the stationary equation (104) for $k = 0$ or $k = \pm\frac{1}{2}$ may exist. Any bifurcations and loops in the energy bands may only occur because of the change in the number of roots of the implicit function (106) which results in the change in the number of negative eigenvalues of the operator L_+.

Numerical evidences in [15] show that the loops of the energy bands are typically centered at the interior points of the Brillouin zone for $k \in (0, \frac{1}{2})$ and these loops originate via the fold bifurcations in the roots of the implicit equation (106). This mechanism is clearly different from the loop bifurcations in the cubic stationary equation (2), where the loops of the energy band cannot be centered at any $k \in (0, \frac{1}{2})$ according to Lemma 1.

7. Conclusion

To summarize, stationary Bloch waves of the Gross–Pitaevskii equation are studied in a periodic potential. It is proved that the stationary real solutions are uniquely continued from the linear limit. Numerical and asymptotic results indicate that the stationary real branch undertakes a bifurcation when an eigenvalue of the linearization operator L_- changes sign in the continuation

with respect to the strength of the nonlinear interactions. The spectrum of L_- is computed numerically to observe this behavior.

The bifurcation of the stationary real branch is studied analytically using the Lyapunov–Schmidt reduction method and is revealed to be a pitchfork (symmetry-breaking) bifurcation. The analysis relies on the normal form equations which expose the qualitative behavior of the system around the bifurcation point. This behavior is illustrated numerically in specific examples.

Finally, the stability of the stationary states is examined. The stationary real branch at the lowest energy band is found to be stable before the bifurcation point after which it loses its stability. The new complex stationary solutions are found to be stable as they appear. The stability of solutions along a loop in the energy band is also established.

References

1. J. C. Bronski, L. D. Carr, B. Deconinck, J. N. Kutz, and K. Promislow, Stability of repulsive Bose-Einstein condensates in a periodic potential, *Phys. Rev. E* 63: 036612 (2001).
2. M. Chugunova and D. Pelinovsky, Count of eigenvalues in the generalized eigenvalue problem, *J. Math. Phys.* 51: 052901 (2010).
3. M. Coles, Bifurcations of Bloch waves in periodic potential, B.Sc. Project, McMaster University, 2011.
4. M. S. Eastham, *The Spectral Theory of Periodic Differential Equations*, Scottish Academic Press, Edinburgh, 1973.
5. E. Kirr, P. G. Kevrekidis, and D.E. Pelinovsky, Symmetry-breaking bifurcation in the nonlinear Schrodinger equation with symmetric potentials, arXiv:1012.3921.
6. C. Kittel, *Introduction to Solid State Physics* (8th ed.), John Wiley & Sons, New York, 2005.
7. M. Machholm, C. J. Pethick, and H. Smith, Band structure, elementary excitatioins, and stability of a Bose–Einstein condensate in a periodic potential, *Phys. Rev. A* 67: 053613 (2003).
8. T. Mayteevarunyoo and B. A. Malomed, Stability limits for gap solitons in a Bose–Einstein condensate trapped in a time-modulated optical lattice, *Phys. Rev. A* 74: 033616 (2006).
9. A. Pankov, Periodic nonlinear Schrödinger equation with application to photonic crystals', *Milan J. Math.* 73: 259–287 (2005).
10. D. E. Pelinovsky, Inertia law for spectral stability of solitary waves in coupled nonlinear Schrödinger equations, *Proc. R. Soc. London, Ser. A* 461: 783–812 (2005).
11. D. E. Pelinovsky, *Localization in Periodic Potentials: From Schrödinger Operators to the Gross–Pitaevskii Equation*, Cambridge University Press, Cambridge, 2011.
12. D. E. Pelinovsky and T. Phan, Normal form for the symmetry-breaking bifurcation in the nonlinear Schrodinger equation, arXiv:1101.5402.
13. L. Pitaevskii and S. Stringari, *Bose-Einstein Condensation*, Oxford University Press, Oxford, 2003.
14. B. Prasanna Venkatesh, M. Trupke, E. A. Hinds, and D. H. J. O'Dell, Atomic Bloch–Zener oscillations for sensitive force measurements in a cavity, *Phys. Rev. A* 80: 063834 (2009).

15. B. Prasanna Venkatesh, J. Larson, and D. H. J. O'Dell, Band-structure loops and multistability in cavity QED, *Phys. Rev. A* 83: 063606 (2011).
16. M. Skorobogatiy and J. Yang, *Fundamentals of Photonic Crystal Guiding*, Cambridge University Press, Cambridge, 2009.
17. B. Wu and Q. Niu, Superfluidity of Bose–Einstein condensate in an optical lattice: Landau–Zener tunnelling and dynamical instability, *New J. Phy.* 5: 104 (2003).
18. J. Yang, *Nonlinear Waves in Integrable and Nonintegrable Systems*, SIAM, Philadelphia, 2010.
19. Y. Zhang and B. Wu, Composition relation between gap solitons and Bloch waves in nonlinear periodic systems, *Phys. Rev. Lett.* 102: 093905 (2009).
20. E. Zeidler, *Applied Functional Analysis: Main Principles and Their Applications*. Springer-Verlag, New York, 1995.

McMaster University

(Received June 27, 2011)